

Review

Mapping Local Climate Zones and Their Applications in European Urban Environments: A Systematic Literature Review and Future Development Trends

Michal Lehnert ¹, Stevan Savić ^{2,*}, Dragan Milošević ², Jelena Dunjić ³ and Jan Geletič ^{4,5}

¹ Department of Geography, Faculty of Science, Palacký University Olomouc, 771 46 Olomouc, Czech Republic; m.lehnert@upol.cz

² Climatology and Hydrology Research Centre, Faculty of Sciences, University of Novi Sad, Trg Dositeja Obradovića 3, 21000 Novi Sad, Serbia; dragan.milosevic@dgt.uns.ac.rs

³ Department of Geography, Tourism and Hotel Management, Faculty of Sciences, University of Novi Sad, Trg Dositeja Obradovića 3, 21000 Novi Sad, Serbia; jelenad@dgt.uns.ac.rs

⁴ Department of Complex Systems, Institute of Computer Science of the Czech Academy of Sciences, 182 07 Prague, Czech Republic; geletic@cs.cas.cz

⁵ Global Change Research Institute of the Czech Academy of Sciences, 603 00 Brno, Czech Republic

* Correspondence: stevan.savic@dgt.uns.ac.rs

Abstract: In the light of climate change and burgeoning urbanization, heat loads in urban areas have emerged as serious issues, affecting the well-being of the population and the environment. In response to a pressing need for more standardised and communicable research into urban climate, the concept of local climate zones (LCZs) has been created. This concept aims to define the morphological types of (urban) surface with respect to the formation of local climatic conditions, largely thermal. This systematic review paper analyses studies that have applied the concept of LCZs to European urban areas. The methodology utilized pre-determined keywords and five steps of literature selection. A total of 91 studies were found eligible for analysis. The results show that the concept of LCZs has been increasingly employed and become well established in European urban climate research. Dozens of measurements, satellite observations, and modelling outcomes have demonstrated the characteristic thermal responses of LCZs in European cities. However, a substantial number of the studies have concentrated on the methodological development of the classification process, generating a degree of inconsistency in the delineation of LCZs. Recent trends indicate an increasing prevalence of the accessible remote-sensing based approach over accurate GIS-based methods in the delineation of LCZs. In this context, applications of the concept in fine-scale modelling appear limited. Nevertheless, the concept of the LCZ has proven appropriate and valuable to the provision of metadata for urban stations, (surface) urban heat island analysis, and the assessment of outdoor thermal comfort and heat risk. Any further development of LCZ mapping appears to require a standardised objective approach that may be globally applicable.

Keywords: local climate zones; urban environment; urban climate; urban heat island; heat load assessment



Citation: Lehnert, M.; Savić, S.; Milošević, D.; Dunjić, J.; Geletič, J. Mapping Local Climate Zones and Their Applications in European Urban Environments: A Systematic Literature Review and Future Development Trends. *ISPRS Int. J. Geo-Inf.* **2021**, *10*, 260. <https://doi.org/10.3390/ijgi10040260>

Academic Editor: Wolfgang Kainz

Received: 8 March 2021

Accepted: 5 April 2021

Published: 12 April 2021

Publisher's Note: MDPI stays neutral with regard to jurisdictional claims in published maps and institutional affiliations.



Copyright: © 2021 by the authors. Licensee MDPI, Basel, Switzerland. This article is an open access article distributed under the terms and conditions of the Creative Commons Attribution (CC BY) license (<https://creativecommons.org/licenses/by/4.0/>).

1. Introduction

Recent decades have seen manifestations of climate change at global and regional scales, including considerable rises in the incidence of extreme temperature spells or events (e.g., heat-waves), especially during the 21st century [1]. Further, projections indicate more frequent and severe heat-waves over the European continent will occur [2,3]. These extreme weather events have increased heat-loads in urban areas [4–6], generally manifesting as higher air and surface temperatures, both day and night, when compared with more natural hinterlands [7]. Thus, today's metropolitan areas, cities and towns are facing changes in the magnitude of extreme temperature events in almost every region of the world, with their

occurrence probably in the order of several times higher than that of only a few decades ago [8,9]. These facts take on yet more importance in the light of demographic projections that posit the continuation of rapid urbanization the 21st century, with approximately 70% of the world's population in urban environments by 2050 [10]. It has been predicted that the urban population will reach nearly five billion people by 2030, with a high probability of an urban expansion of possibly 1.2 million km², which constitutes an increase of 185% in global urban area over the year 2000 [11]. Thus, the need for comprehensive research into urban climates and environments is becoming ever more pressing [12].

Given the outline of conditions presented above, it follows that city populations are often at heat-related risk. Several studies indicate that heat stress is becoming more frequent, with associated increases in hospitalization and mortality among vulnerable groups, such as people with pre-existing chronic complaints (e.g., cardiovascular and/or respiratory diseases), children (under the age of 18) and the elderly (those aged 65 and over) [13–17]. Furthermore, Wouters et al. [18] predicted that the increases in heat stress in certain large European cities will be double those in their natural surroundings by 2050. Further, according to a European Commission report [19], deaths attributable to climate change will rise significantly over the next 90 years across the (then) 27 EU countries. It cannot be ignored that cities are of the drivers of global and regional economies, and current temperature extremes may well endanger economic structures and contribute to budgetary problems in cities [20].

More detailed consideration of the heat burden in urban areas tends to focus on their higher proportion of artificial/impervious surfaces (concrete, asphalt, glass, etc.), concentrated human activity resulting in modified radiation and energy-exchange processes, anthropogenic heat fluxes, and reduced evapotranspiration compared to non-urban landscapes [21]. All of these result in higher temperatures in urban areas, a phenomenon known as the “urban heat island” (UHI), or “surface urban heat island” (SUHI). UHI and SUHI are evident not only in large- and mid-sized cities [22–27], but also in smaller cities and in conurbations with fewer than 10,000 inhabitants [22,28–30]. However, temperature conditions are not the same in all areas of a city [31]. Quite apart from considerations of relief [32], they arise out of the dominant surface types, urbanization density, roughness of structural materials, the types of activity undertaken by the inhabitants, and more. Thus, some urban areas may be generally characterised by warmer (or cooler) conditions than others.

In order to frame and define the heat load processes at micro- and local scales within urban areas, the Canadian geographers Stewart and Oke [33] introduced the concept of “local climate zones” (LCZs). This concept has been evaluated with field-work research and experience acquired from such previous classifications as, for example, Ellefsen's [34] scheme of urban terrain zones (UTZs) and by Oke's [35–37] urban climate zones (UCZs).

The authors gathered quantitative data, both measured and estimated (geometric, surface cover, thermal, radiative, metabolic), and qualitative attributes (materials, texture, morphology) related to urban and rural areas world-wide. These served to characterize surface-cover properties in built-up and land-cover zones. The derived considerations of a quantitative nature and of urban design (which provides qualitative attributes) databases are presented in publications addressing urbanization structures and development processes at global/continental/regional levels. These have been published over a 30-year period [34,35,38–48].

The main goal of the new climate-based LCZ classification system for urban and rural areas is to provide a research framework for UHI studies and to standardise the principles of urban (temperature) observations around the world [33]. LCZs are defined as regions with uniform surface cover, urbanization structure, building materials, traffic and human activity features, the areas of which vary from hundreds of square metres to several kilometres on a horizontal scale. It is worthy of note that the LCZ classification system was not basically developed for mapping the UHI effect but to assist in the selection of locations for local weather stations and to report in a standardised manner on the heat-

island effect beyond the urban-rural dichotomy. However, it follows that such a system is also useful in discriminating between climatically distinguishable areas within an urban agglomeration, and also serves to help identify the probable local warming effects of urban development [49].

Stewart and Oke [33] established 17 standard classes of LCZ, in which the first ten represent “built-up” types (from LCZ 1 to LCZ 10) and the other seven characterise “land cover” types (from LCZ A to LCZ G) (Figure 1). The names of built-up LCZs classes are largely indicative of the density of construction (compact/open) and the height of buildings (high-rise/midrise/low-rise). Each LCZ exhibits a distinctive local screen-height temperature regime, at its most apparent over dry surfaces, on calm, clear nights, and in areas of simple relief. The surface structure (height and spacing of buildings/trees) and surface cover (impervious/pervious) have significant influences on screen-height temperatures in LCZs. Surface structure affects local climate through modification of airflow, atmospheric heat transport, and short-wave/long-wave radiation balances, while surface cover modifies the albedo, moisture availability, and heating/cooling potential of the ground [33]. Therefore, a range of geometric and surface-cover values is specified for each LCZ (Stewart and Oke [33]), together with values for thermal, radiative, and metabolic properties (Stewart and Oke [33]).

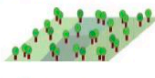
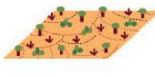
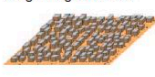
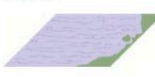
Built types	Definition	Land cover types	Definition
 1. Compact high-rise	Dense mix of tall buildings to tens of stories. Few or no trees. Land cover mostly paved. Concrete, steel, stone, and glass construction materials.	 A. Dense trees	Heavily wooded landscape of deciduous and/or evergreen trees. Land cover mostly pervious (low plants). Zone function is natural forest, tree cultivation, or urban park.
 2. Compact midrise	Dense mix of midrise buildings (3–9 stories). Few or no trees. Land cover mostly paved. Stone, brick, tile, and concrete construction materials.	 B. Scattered trees	Lightly wooded landscape of deciduous and/or evergreen trees. Land cover mostly pervious (low plants). Zone function is natural forest, tree cultivation, or urban park.
 3. Compact low-rise	Dense mix of low-rise buildings (1–3 stories). Few or no trees. Land cover mostly paved. Stone, brick, tile, and concrete construction materials.	 C. Bush, scrub	Open arrangement of bushes, shrubs, and short, woody trees. Land cover mostly pervious (bare soil or sand). Zone function is natural scrubland or agriculture.
 4. Open high-rise	Open arrangement of tall buildings to tens of stories. Abundance of pervious land cover (low plants, scattered trees). Concrete, steel, stone, and glass construction materials.	 D. Low plants	Featureless landscape of grass or herbaceous plants/crops. Few or no trees. Zone function is natural grassland, agriculture, or urban park.
 5. Open midrise	Open arrangement of midrise buildings (3–9 stories). Abundance of pervious land cover (low plants, scattered trees). Concrete, steel, stone, and glass construction materials.	 E. Bare rock or paved	Featureless landscape of rock or paved cover. Few or no trees or plants. Zone function is natural desert (rock) or urban transportation.
 6. Open low-rise	Open arrangement of low-rise buildings (1–3 stories). Abundance of pervious land cover (low plants, scattered trees). Wood, brick, stone, tile, and concrete construction materials.	 F. Bare soil or sand	Featureless landscape of soil or sand cover. Few or no trees or plants. Zone function is natural desert or agriculture.
 7. Lightweight low-rise	Dense mix of single-story buildings. Few or no trees. Land cover mostly hard-packed. Lightweight construction materials (e.g., wood, thatch, corrugated metal).	 G. Water	Large, open water bodies such as seas and lakes, or small bodies such as rivers, reservoirs, and lagoons.
 8. Large low-rise	Open arrangement of large low-rise buildings (1–3 stories). Few or no trees. Land cover mostly paved. Steel, concrete, metal, and stone construction materials.	VARIABLE LAND COVER PROPERTIES	
 9. Sparsely built	Sparse arrangement of small or medium-sized buildings in a natural setting. Abundance of pervious land cover (low plants, scattered trees).	Variable or ephemeral land cover properties that change significantly with synoptic weather patterns, agricultural practices, and/or seasonal cycles.	
 10. Heavy industry	Low-rise and midrise industrial structures (towers, tanks, stacks). Few or no trees. Land cover mostly paved or hard-packed. Metal, steel, and concrete construction materials.	<i>b. bare trees</i>	Leafless deciduous trees (e.g., winter). Increased sky view factor. Reduced albedo.
		<i>s. snow cover</i>	Snow cover >10 cm in depth. Low admittance. High albedo.
		<i>d. dry ground</i>	Parched soil. Low admittance. Large Bowen ratio. Increased albedo.
		<i>w. wet ground</i>	Waterlogged soil. High admittance. Small Bowen ratio. Reduced albedo.

Figure 1. Built and land-cover types in Stewart and Oke’s [33] local climate zone (LCZ) classification system. Source: Stewart and Oke [33].

The concept of LCZs contributed to a progressive step in the thermal analysis of urban areas. Thermal differences (in UHI/SUHI intensities, for example) were no longer confined to urban/rural temperature differences, but could also focus more closely on the differences between LCZs. Thus, the LCZ system provides an approach to the comparison of the thermal features of various neighbourhoods/areas within a city (“intra-urban analysis”), and/or comparison of similar types of neighbourhoods/areas between cities (“inter-urban analysis”) [50,51].

The concept of LCZ classification has found wide acceptance and application in a range of urban climate investigations. This review study is therefore intended to provide an overview of the concept and context of articles that have applied the LCZ classification system. To date, no other study has presented a comprehensive analysis of the methods of detection and mapping of LCZs and their application to thermal assessments in European cities and urban areas. A number of review studies have appeared, but they have focused on only certain segments of the analysis of LCZs, such as remote sensing-based methods [52] or the application of the MUKLIMO_3 model [53]. In this systematic review study [54], we put attention complexly on LCZs studies in European environment. Attention was devoted primarily to the following goals: (a) collecting existing LCZ-related studies covering the European urban environment (over the last 8.5 years, i.e., 2012–2020) using a precisely-defined search methodology; (b) analyzing and presenting the context and methods of LCZ detection and delineation/mapping contained within them; (c) summarizing the results of studies monitoring and modelling meteorological/climatological values (largely thermal) within the methodological framework of LCZs; and (d) discussing the importance and limits of LCZs for contemporary and future urban climate research.

2. Search Methodology

This section presents in detail the whole approach to a systematic search for, and analysis of, studies directly associated with the application of the concept of LCZs. The investigation was carried out by collecting, reviewing and analyzing scientific articles, and the process included three phases:

- Literature selection.
- Context and content analysis.
- Classification of the articles obtained according to two sets of criteria.

2.1. First Phase: Literature Selection

Definition of keywords was an obvious initial step. Since the concept of LCZs and its application is the main focus of this review study, “local climate zones” was selected as the main keyword phrase, appearing in that form article titles, lists of keywords or in abstracts. The term “urban heat island” was then added to the search, combined with the term “local climate zones”. Two academic research databases, WoS (Web of Science) and Scopus, were used to seek and extract the relevant scientific articles. Since the concept of LCZs (by that exact name) emerged in 2012, the search was limited to the period between 1 January 2012 and 30 June 2020.

The literature selection process consisted of five steps:

The first step of the review process resulted in a similar number of results from both databases: 316 articles from WoS and 314 articles from Scopus.

The second step of the review included the application of two filters to both databases in order to identify the articles that lay within the scope of this review. In the first, the search was limited to the European area; case studies from other continents were excluded. The second filter step involved the type of article, limiting the search to only research articles, review articles and in-press articles (early access), while conference papers, notes, editorials, etc. were excluded. These filters resulted in considerably fewer articles: 86 from WoS and 90 from Scopus.

The third step was to screen the articles obtained in terms of title and abstract before exporting the data from the WoS/Scopus websites. This served to exclude articles from non-

European countries for which the WoS/Scopus algorithms had failed to define location for our purposes. Some articles were not related to the LCZ concept at all, and were excluded. This step left 68 articles from WoS and 76 from Scopus. The majority of articles matched in both databases; those differences that did occur were largely confined to journals indexed in Scopus, but not in WoS. Joining the two databases and excluding matching articles (duplicates) returned 103 articles to be taken into account for further analyses.

The fourth step screened Title/Abstract/Method, to identify the studies that merely mentioned LCZs rather than actually applying them. This led to the exclusion of a further eight articles, so the 95 remaining articles were considered potentially relevant.

In the fifth and final step, seven articles obtained from the WoS/Scopus databases were excluded because they were already works of screening and reviewing. At the very end, using the “snowballing method” [55], three articles obtained from the bibliographies of the fully-reviewed articles were included into the final list of the 91 articles identified as relevant for this analysis (Supplementary Materials Table S2). The whole process is illustrated in the work flow-chart (Figure 2).

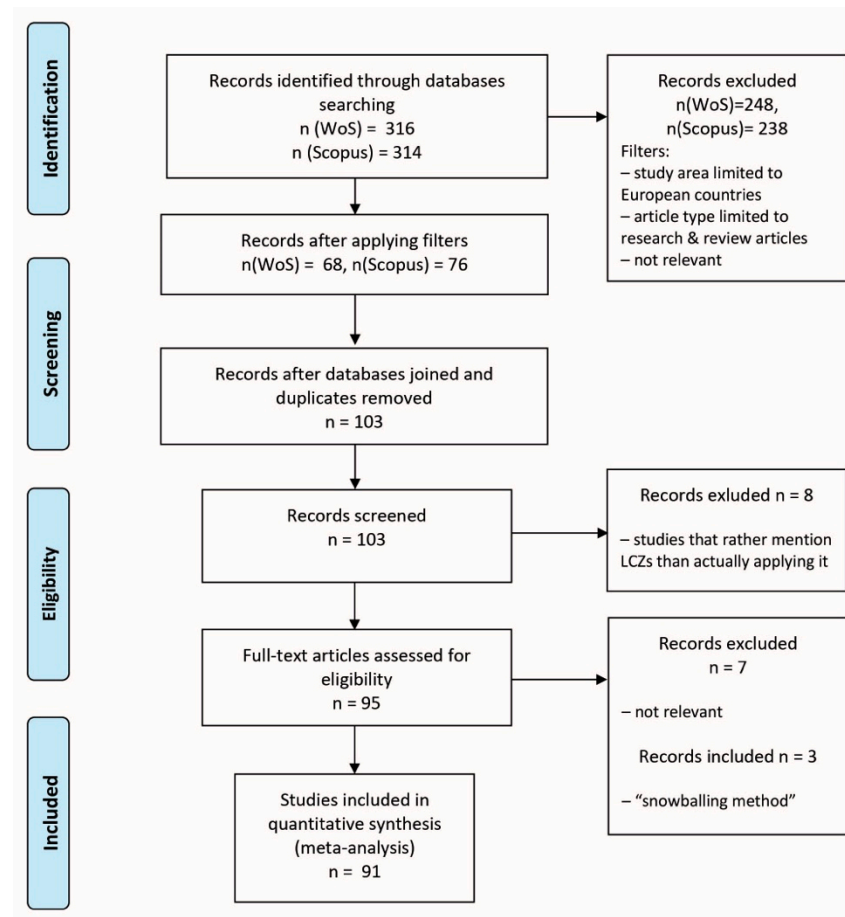


Figure 2. Flow-chart of the literature selection and review process using initial keywords and WoS/Scopus databases [56].

2.2. Second Phase: Context and Content Analysis

Several aspects of the context and content of LCZ studies relevant to this review were analysed by means of VOSviewer software (1.6.13). This is considered a useful tool in the analysis and visualisation of bibliographical data. It provides a clear overview of the main areas covered by the selected articles, as well as of the development over time of the field [57–59]. The software supports the data obtained from the WoS and Scopus databases, but simultaneous analysis is not possible, so the analysis and visualization were performed separately for each database. Prior to data visualization, the database was prepared in a

fashion similar to that employed in the literature selection process. Firstly, the key phrase “local climate zones” was separately sought in the search engines of the databases, then the filters regarding geographical scope and article type were applied, and the process ended after the first-phase screening (immediately within the search engines in WoS/Scopus).

Before analysis began, thesaurus files that contained similar terms and words (e.g., author names and initials of the same authors) were created in order to merge them with near-identical terms. For example, terms such as “local climate zone”, “local climatic zones” and “LCZ” were merged with the term “local climate zones” in order to avoid distraction in the analysis arising out of the occurrence of more terms than there really are. Such analyses facilitated disclosure and discussion of the thematic areas of LCZ delineation and application in European urban spaces.

The results were analysed according to the following criteria:

- Authors’ key word co-occurrence in the selected articles from WoS and Scopus.
- The most common sources of LCZ-related articles and the citation links between them from WoS and Scopus.
- The most-cited sources of LCZ-related articles and the citation links in WoS and Scopus.
- The geographical extent of the studies identified (areas studied).

Detailed results appear in Section 3.1 (Context and content of LCZ studies).

2.3. Third Phase: Classification of LCZ Studies

The final stage of the review process included screening and review of full articles, according to two sets of criteria.

The first criterion was based on classification of LCZ research articles based on the methods of LCZ mapping employed, i.e., detection and delineation of various urban/non-urban surface morphologies (Section 3.2). These classes were:

- Expert knowledge-based method. This refers to the definition of LCZs based on author(s)’ expertise and local knowledge of given urban/hinterland areas, or on author(s)’ judgement based on general urban surface calculations that are not explained in detail in the publication.
- GIS-based method. This presents the calculations of relevant parameters for LCZs definition by the exclusive use of Geographic Information System (GIS) tools or platforms.
- Remote sensing imagery-based method. This indicates reliance on remote-sensing datasets (e.g., satellite images) and the employment of one or more methods to land-cover feature calculations from imagery in order to define LCZs.
- Combined method. This specifies that at least some part of the definition of LCZs was based on clearly-defined values of geometric, surface cover, thermal radiative and metabolic properties, and that the previously-mentioned methods are evenly combined for these surface/thermal calculations.

The second criterion divided the LCZ research articles on the basis of a combination of the main aims of the analysis, or the main purpose of employment/application of the concept of LCZs (Section 3.3). It is presented herein by the following classes:

- Thermal analysis based on in-situ measurements.
- Thermal analysis based on mobile measurements.
- Thermal analysis based on land-surface measurements.
- Thermal analysis based on modelling approaches.

Such contextual and methodological analyses of LCZs studies enable the summarization and systematic discussion of the LCZ concept and its role in urban climate research in the European urban environments, a matter that has not to date been comprehensively addressed.

3. Results

3.1. Context and Content of LCZ Studies

The number of studies addressing LCZs or employing the LCZ concept is rising continuously. However, the aims of the studies, as well as the way in which LCZs are being used, are changing. At the beginning of the review period, LCZ investigations were largely directed towards its application in the classification and detection of urban meteorological station measurement sites, using expert- and GIS-based knowledge. Later, LCZ researchers became engaged in studying spatial and temporal patterns of air temperature and the application of LCZs in urban climate modelling (in 2019 and 2020), largely on the basis of remote sensing databases (Figure 3).

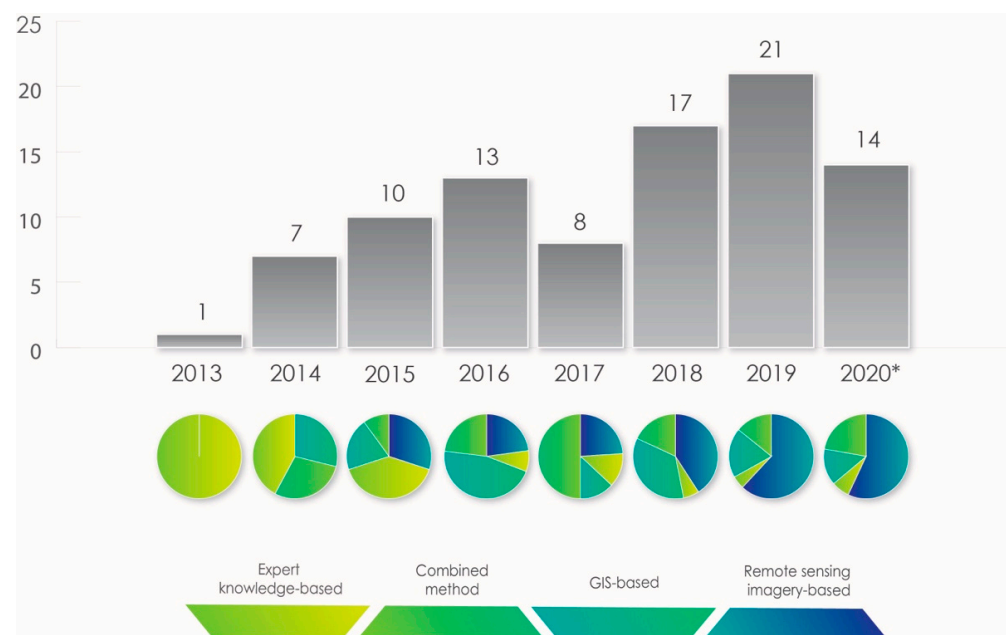


Figure 3. Time distribution of studies based on the methodological and conceptual uses of LCZ classification; (Note: 2020-studies published by July 2020).

More detailed key-word analyses show that “local climate zones” have already become firmly established in urban climate research, particularly in studies related to the urban heat island effect (Figure 4, A1/A2). More precisely, “local climate zones” and “urban climate” have frequently been used together as keywords since 2012, the year in which the completed concept of LCZs was published [33]. Thereafter, this was reflected or employed in a number of urban climate research studies. Later on, the association of LCZs with “urban heat island” and “air temperature” became pronounced. It is also noteworthy that, in the articles published in 2016, the main keywords associated with local climate zones were “urban geometry”, “urban planning”, “monitoring”, “computational fluid dynamics”, “boundary layer meteorology”, and “GIS”. From 2017 onwards, other keywords, such as “ENVI-met”, “land use/land cover”, and “Landsat” frequently emerged together with “local climate zones”. From 2018 onwards, keywords such as “heat wave”, “outdoor thermal comfort”, “remote sensing”, “urban cold island”, and “urban green spaces” occur. In 2019 and 2020, more keywords related to “satellite imagery”, “land cover mapping”, “spatial analysis”, and “convolutional neural networks” appear.

Such results illustrate a shift in LCZ-related research interest towards its applied usage in urban areas with respect to urban heat island phenomena, urban planning and design, GIS applications, remote sensing, and more. This focus then shifted towards investigation of extreme events such as heat waves, assessing outdoor thermal comfort in urban areas, mitigation strategies (e.g., urban green spaces), all applying remote sensing as a common means of investigation. The latest research is still more reliant on satellite data, mapping

Nevertheless, it is also worth mentioning the relatively high number of methodologically-based research articles throughout the period investigated. This indicates a certain inconsistency of approach towards the concept of LCZs, as well as a sense on the part of researchers that the LCZ concept (especially methods of LCZs delineation) might be further improved.

As is evident in Figure 4, the results from the two databases provided similar outputs with respect to the most frequently used keywords, as well as the time-lines of their appearance. This is hardly surprising, given that a high number of articles matched in both databases. The main difference between the articles that appeared in WoS and those from Scopus was that some journals are not indexed in the WoS database, among them the “Hungarian Geographical Bulletin” journal. The analysis of the article sources, as well as the cited sources, differs slightly for the two databases. In both of them, most of the articles are published in the journals *Urban Climate* and *Theoretical and Applied Climatology*. However, the *Hungarian Geographical Bulletin* is not indexed in WoS, although it appears in Scopus; a significant number of articles regarding the application of the concept of LCZs have been published in this journal, and many other publications are cited in it. This journal is therefore highly-positioned according to the number of published articles in journals indexed in Scopus (Supplementary Materials Figure S1).

The situation is different for the average number of citations, i.e., the sources of articles with higher average citation scores are slightly different in the two databases, as are the connections between them, which results in slightly different visual presentations (Supplementary Materials Figure S1). In both databases, articles published in the *IEEE Journal of Selected Topics in Applied Earth Observations, Remote Sensing and Landscape and Urban Planning* are the most frequently cited by other articles published in further journals. Of the Scopus-indexed journals, more prolifically-cited articles are published in *Meteorologische Zeitschrift* and *Atmosphere* journals. In contrast, significantly-cited articles from WoS-indexed journals tend to be published in *Remote Sensing*.

This contribution takes into consideration only articles in which the study area lay within Europe. Geographical analysis of the European urban study areas revealed which urban environments were most often investigated in terms of the LCZ concept (Figure 5). In a number of studies, analyses took in ten or more cities at once, in one or more European countries, and some did not address all the cities in detail, but showed only general LCZ patterns. This was the situation for 42–100 cities in France [59–61], 235 cities in Bulgaria [62], from ten to a few dozen cities across Europe [52,63–66]. Cities from those articles do not, therefore, appear in Figure 5.

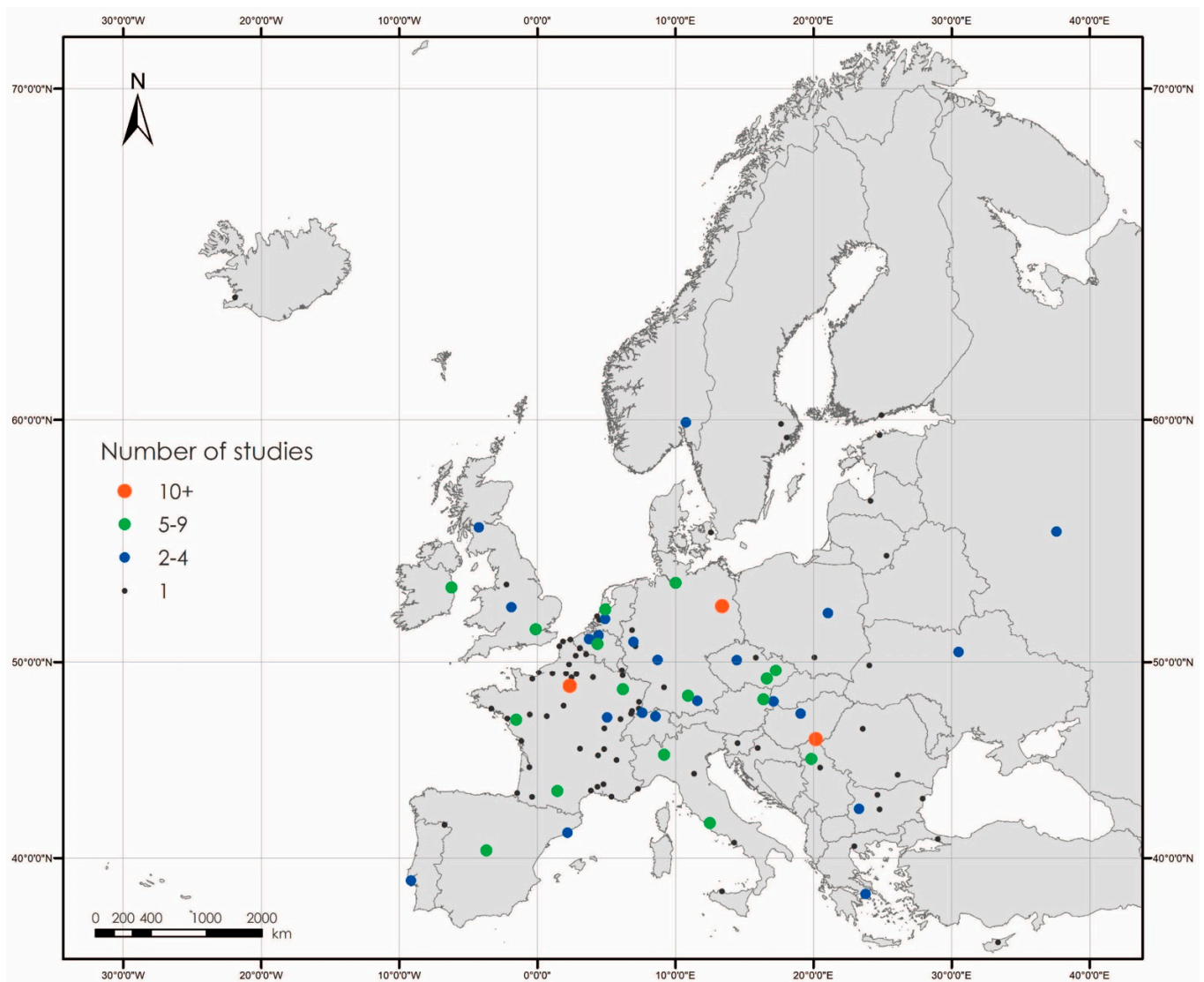


Figure 5. Geographical extent of the study areas identified within Europe.

3.2. Methods of LCZ Detection and Delineation

Even before the publication of the final version of the LCZ classification concept [33], LCZs had been addressed in terms of regional typology by [67], with Bechtel and Daneke [68] providing the specific, climate-related, land use/cover typology. Unger et al. [67] identified and mapped LCZs in the city of Novi Sad (Serbia), using expert-knowledge-based methodology to define appropriate measurement sites for the urban meteorological network and to provide intra-/inter-urban thermal analysis for further research. Bechtel and Daneke [68] used a satellite imagery-based method to define LCZs in the urban area of Hamburg (Germany). They employed pixel-based classification approaches, relying on multiple satellite and airborne earth observation data of the built-up environment and a range of classifiers. Their objective was to facilitate an automated classification of LCZs. In both the above contributions, the authors referred to the work undertaken by Stewart and Oke and presented before 2012 at international conferences [69,70].

Most of the studies reviewed utilised urban-cover geometric/surface elements, as well as thermal/radiative/metabolic elements, as defined by Stewart and Oke [33] for the detection and mapping of LCZs. In the subsections below (from Sections 3.2.1–3.2.4), the selected publications are organized into four different classes on the basis of the methods applied for the detection and delineation of LCZs. Figure 6 presents the number of studies based on each method. However, it is important to note that there is no absolute definition

involved in the categorisation. This can only be determined in a conceptual/theoretical manner, since there are no strict criteria for what constitutes, for example, a solely GIS-based method, or remote sensing-based or expert-based knowledge, etc. LCZ classification approaches frequently overlap to a greater or lesser extent.

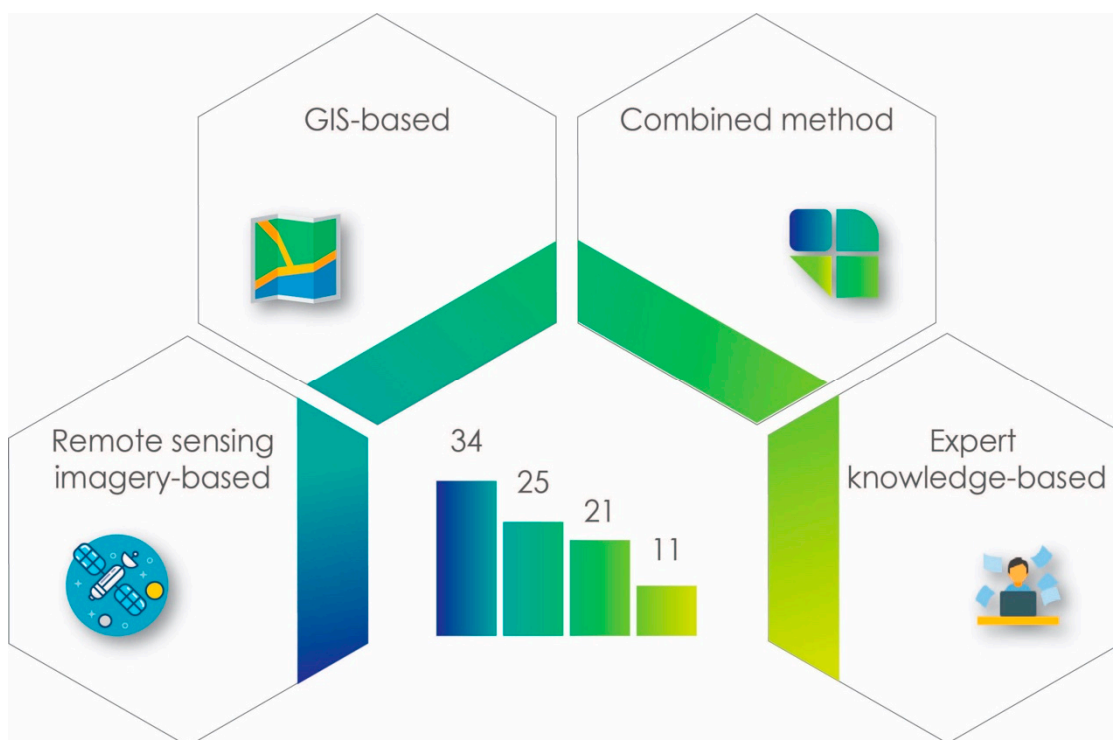


Figure 6. Distribution of studies by methods employed for the detection and delineation of LCZs.

3.2.1. Expert Knowledge-Based Method

LCZ research based on expert local/researcher knowledge has a strong tendency to focus on the definition of metadata from specific station sites that are part of an urban meteorological network (UMN). These measurement points depict conditions in micro- or local locations. In such cases, local knowledge of the given urban morphology is crucial to optimizing the accuracy of LCZ detection. Stewart and Oke [33] were at pains to point out that each LCZ has a specific temperature footprint and the precise definition of LCZs at measurement sites is crucial to gathering real, measured datasets. Therefore, in the course of detecting LCZs, researchers incorporate certain vital elements into their assessments. These include surface characteristics, such as local building geometry, land cover, aerial photographs, satellite images (e.g., Google Earth), the width of streets, spatial patterns of trees and green patches, and other geometric, thermal, radiative, metabolic, and terrain roughness lengths properties/datasets, as defined by Stewart and Oke [33] and Davenport et al. [71].

Based on expert-based method and morphology datasets, Savić et al. [72] defined 28 station locations in nine LCZs, covering the urban and hinterland areas of Novi Sad (Serbia), for a future UMN. Lehnert et al. [25] used a combination of GIS-based analyses and field research, together with calculations of geometric and surface cover properties, to define the 14 stations of the UMS in Olomouc (Czech Republic) in terms of local climate zones. In Germany, a combination of research expertise and surface morphology datasets from city administrative sources was incorporated into the LCZ methodology employed for assessments of six measurement sites in Hamburg (HUSCO network) [73] and eight stations in Oberhausen [74]. Explicit consideration of the geometric and surface properties, as defined in the definitive LCZ study [33], served to classify the LCZs as fixed measure-

ment sites [75], while mobile measurement traverses formed the basis of urban climate research in Cluj-Napoca (Romania) [75] and Uppsala (Sweden) [50]. Pour et al. [76] and Pour and Voženílek [77] personally delineated and visualized the most common LCZs in Olomouc (Czech Republic) by combining local expert knowledge and Urban Atlas classification with airborne thermal remote-sensing datasets to assess the thermal regime of a range of urban patterns. An alternative approach, addressing urban thermal and wind modelling, was taken in the definition of ten built-up LCZs in Basel (Switzerland) by Theeuwes et al. [78] and Droste et al. [79]. They employed expert knowledge in the assessment of various urban parameters (surface emissivity, albedo, roughness length, building height, anthropogenic heat, vegetation fraction, and initial boundary-layer height). Finally, Tornay et al. [60] developed the “GENERator of Interactive Urban blocks” (GENIUS) typology for French cities, which parallels the ten classes of built-up LCZs. GENIUS is based on constructing “archetypes” that embody urban typology, building use, construction date, and geographical location (Table 1).

Table 1. Expert knowledge-based methods for mapping LCZs, as derived for the purposes of review.

Method Used	Study	City/Region Analysed	LCZ Classes Detected
Expert assessment for UMN	[72]	Novi Sad (Serbia)	2, 3, 5, 6, 8, 9, 10, A, D
	[25]	Olomouc (Czech Republic)	2 _{CC} , 2 _{BOC} , 4, 4 ₂ , 5, 5 ₆ , 6, 6 ₅ , 9 ₅ , B _D , B _{DW}
	[73]	Hamburg (Germany)	2, 6, D
	[74]	Oberhausen (Germany)	2, 5, 6, 8, 9, A, D
Expert assessment for UMN/mobile measurements	[75]	Cluj-Napoca (Romania)	1, 2, 3, 6, 8, 9, B
Expert assessment of sites on mobile measurements route	[50]	Uppsala (Sweden)	2, 5, 9, D
Expert assessment plus Urban Atlas classes	[76]	Olomouc (Czech Republic)	2, 4, 5, 6, 8, A, G
	[77]		
Expert assessment plus urban parameters	[78]	Basel (Switzerland)	1–10
	[79]		
GENIUS typology	[60]	French cities	1–10

3.2.2. GIS-Based Method

GIS-based methods for the classification and mapping of LCZs have been, by and large, confined to the cities of central Europe. Two GIS-based approaches have emerged, that of Lelovics et al. [51] and that of Geletič and Lehnert [80].

The Lelovics-Gál GIS-based method was first deployed in the delineation and mapping of LCZs in Szeged (Hungary) [26,51,81] and Novi Sad (Serbia) [26], in the LCZ definition of station locations (with T_a and RH sensors) for UMN in the two cities [82,83]. It has also been employed for urban thermal assessments [26,84–91] and heat-risk estimation [92]. The method refines data to a micro-scale. The basic unit is a “lot area polygon”, a term that encompasses a building and its immediate surroundings. A range of inputs is required for this kind of spatial calculation, among them the building database (building footprints), aerial photographs, topographical maps (1:10,000 or 1:25,000), a road database, and Corine Land Cover and Satellite images (at high resolutions). These datasets are used to calculate the geometric and radiative properties as defined by Stewart and Oke [33]: sky-view factor, building height, surface roughness, surface albedo, NDVI (Normalized difference vegetation index), building surface fraction and impervious/pervious surface fractions. This method can satisfactorily classify all ten built-up classes, but has the drawback that it is not suitable for detection of land-cover classes (local researcher expertise required). The LCZ class for any given area polygon is determined after automated calculation of the parameters listed. In order to make LCZ maps more accessible in the light of the number of lots involved (e.g., 47,000 lot area polygons were determined for the Novi Sad urban area),

an aggregation process is activated in which identical or similar LCZ classes are merged into a zone with a radius of ≥ 250 m (Figure 7).

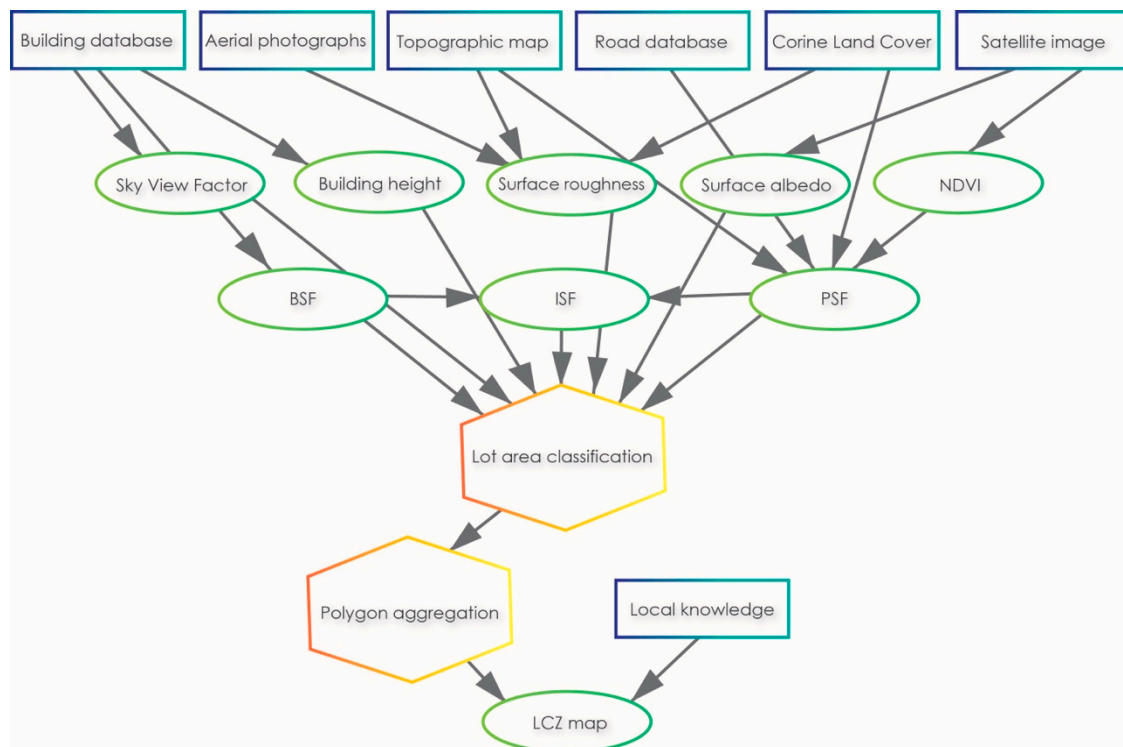


Figure 7. Flow-chart of the GIS-based method, after Lelovics et al. [51]. Source: Unger et al. [81] (published by Hungarian *Geographical Bulletin*, 2014, 63, 29–41, doi:10.1520L/hungeobull.53.1.3 f). Note: NDVI—normalized difference vegetation index; BSF—building surface fraction; ISF—impervious surface fraction; PSF—previous surface fraction.

The Geletič-Lehnert GIS-based method [80] relies on those Stewart and Oke’s [33] physical surface properties of the urban environment that are accurately measurable and clearly defined decision-making algorithm. This method makes it possible to calculate four surface parameters: building surface fraction (BSF), impervious surface fraction (IFS), previous surface fraction (PFS), and height of roughness elements (HRE). The novelty of this method lies in its implementation of one more parameter: the number of buildings (NoB) per hectare. Furthermore, an additional six parameters are defined and calculated (number of areas in which the continuous surface of tree-crown cover stands above 2 m, number of continuous fragments of all vegetation per hectare, surface covered by high vegetation, surface covered by low vegetation, surface covered by bare ground, surface covered by water; all the latter serve to differentiate between specific built-up and land-cover LCZs. The classification process consists of dividing all the urban areas into grid cells of 100×100 m², each of them conforming to defined physical parameters. The methodological procedure of the Geletič-Lehnert GIS-based method consists of four steps: (a) preparation of input data; (b) classification procedure; (c) filtering and post-processing; and (d) validation and comparison. Finally, the reported accuracy of the classification ranges from 87% to 90% [93]. To date, this GIS-based method has been applied largely to cities in the Czech Republic [5,80,93–98] and Serbia [93]. However, non-validated data for some other (world) cities are also freely available.

A few individual studies have developed and/or applied other GIS-based methods for LCZ mapping, in contrast to the two more widely-used approaches mentioned above. For example, Bocher et al. [61] developed a geoprocessing framework for the computation of urban indicators, using three scales as potential input for LCZ mapping of French cities. Rodler and Leduc [99] also developed a GIS-based method of classifying LCZs at

local/micro-scales in selected areas of Nantes (France), using two vector-based algorithms integrated into open-source GIS. A GIS-based method consisting of a vector-based reclassification scheme has been used for LCZ mapping of southern European cities, designed to translate Copernicus datasets into LCZs. It employs the Urban Atlas and Corine Land Cover data for reclassification steps [100] (Table 2).

Table 2. GIS-based methods for LCZ mapping, as derived for the purposes of review.

Method Used	Study	City/Region Analysed	LCZ Classes Detected
GIS-based (Lelovics-Gál)	[51]	Szeged (Hungary)	2, 3, 5, 6, 8, 9, 10, A, B, C, D, G
	[81]		
	[84]		
	[85]		
	[86]		
	[88]	Szeged (Hungary); Novi Sad (Serbia)	
	[89]		
	[90]	Novi Sad (Serbia)	2, 3, 5, 6, 8, 9, 10, A, D, G
	[91]		
	[26]		
	[82]		
	[87]		
	[92]		
	[83]		
GIS-based (Geletič-Lehnert)	[80]	Brno; Prague; Olomouc; Hradec Králové (Czech Republic)	1, 2, 3, 4, 5, 6, 8, 9, 10, A, B, C, D, E, F, G (Brno)
	[94]		2, 3, 4, 5, 6, 8, 9, 10, A, B, C, D, E, F, G (Prague)
	[5]		1, 2, 3, 4, 5, 6, 8, 9, 10, A, B, C, D, E, F, G (Olomouc)
	[98]		2, 3, 4, 5, 6, 8, 9, 10, A, B, D, E, G (Hradec Králové)
	[95]		2, 3, 4, 5, 6, 7, 8, 9, 10, A, B, C, D, E, F, G (Novi Sad)
	[96]		
	[97]		
	[93]		
Open geoprocessing framework	[61]	French cities	1, 2, 3, 4, 5, 6, 7, 8, 9, 10
GIS-Delaunay triangulation/Skeleton-ization	[99]	Nantes (France)	All 17 LCZs
Alternative GIS-based method	[100]	Athens (Greece); Barcelona (Spain); Lisbon (Portugal); Marseille (France), Naples (Italy)	All 17 LCZs

3.2.3. Remote Sensing Imagery-Based Method

In seeking universal methods to quantify the various urban and non-urban surface types for further spatial thermal assessments, analysis of remote sensing data derived from satellite and airborne surface observation, as well as the use of imagery-based processing, may well prove the most widely applicable approach [68]. The World Urban Database and Access Portal Tools (WUDAPT) project was created to facilitate the employment of such knowledge (available at: <http://www.wudapt.org/> [101], accessed on 15 December 2020). It has been presented in a number of studies [52,66,102,103]. The general goals of the WUDAPT project are to: (a) gather and disseminate information about urban/non-urban surfaces and morphologies around the globe, and to contribute in LCZ classification processes; and (b) to provide tools for the investigation of built-up and land-cover properties at scales appropriate to various aspects of climate, weather, the environment and administrative planning [103]. To this end, WUDAPT is intended to provide a universal, simple mapping method that allows local experts, without experience of remote sensing processing or GIS tools, to establish and validate an LCZ classification for any given city and its

hinterland. Surface/object analysis using the WUDAPT method is based on the complexity of detail, as defined at three levels: (a) Level L0—covers regional or city scales (resolution 100–500 m²), and results in urban/land cover maps of LCZ classification described in two-dimensional forms, using satellite and Google Earth sources. Thus, L0 level products contain basic information about urban surfaces; (b) Level L1—covers the neighbourhood scale (resolution 100–500 m²) with 2.5-dimensional presentation of urban morphologies and functions obtained from LCZ maps (derived from the L0 level) and presenting surface/object parameters in more localized detail. At the L1 level, the data are gathered from a range of sources (satellite images, Google Earth, local data, expert knowledge); and (c) Level L2—presents three-dimensional urban forms and building data at very fine resolution, 2 m² (building scale), using satellite and urban databases. Thus, L1 and L2 products provide more detailed information about urban areas, at higher resolution [103].

The L0 level of the WUDAPT method (Figure 8) was used in the detection and delineation of LCZ classes in most of the studies reviewed herein. LCZs maps obtained from L0 may be considered key inputs for further thermal intra-/inter urban assessments and urban climate modelling [52]. Bechtel et al. [52,102] presented the protocol for the WUDAPT L0 method in terms of its capacity to provide standardised physical properties of urban/non-urban surfaces, then to use freely-available data and software, easily put to use without special knowledge of satellite image processing or the use of GIS tools. The final quality of the L0 products depends largely on the skills and experience of the expert/researcher at the first and second steps of processing.

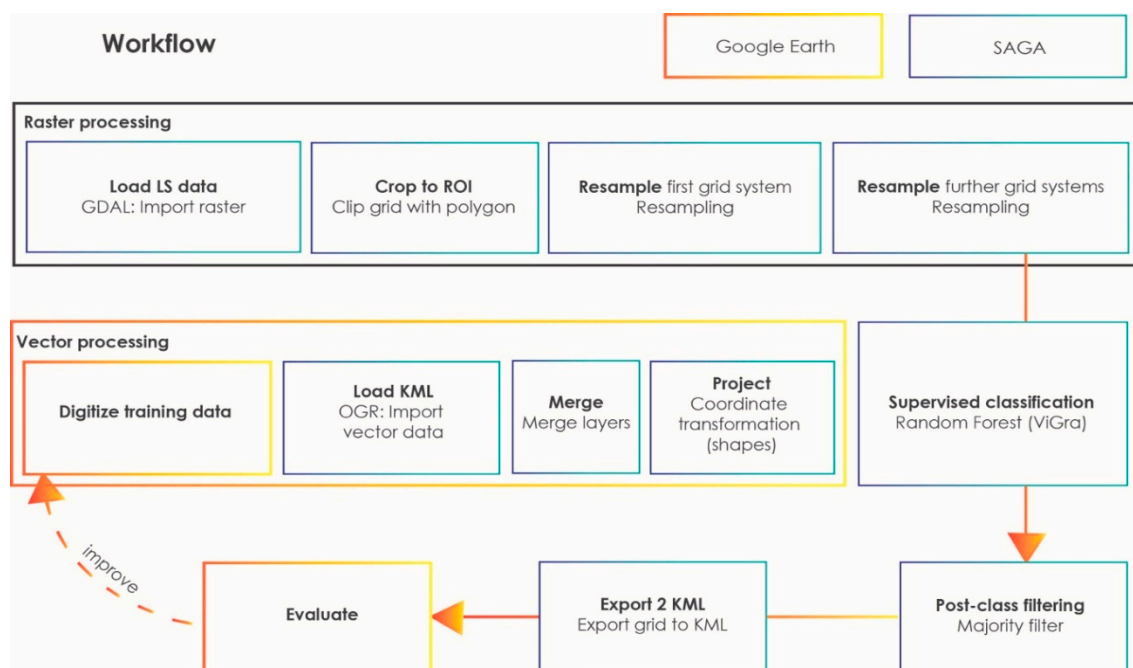


Figure 8. Flow-chart of the L0 level within the WUDAPT method, as presented by Bechtel et al. [102]. Source: Bechtel et al. [52,102].

The first step consists of pre-processing the open-source Landsat-8 satellite OLI-TIRS scenes (raster data) in the system for automated geoscientific analysis (SAGA-GIS) software [104]. This involves cropping the data to the region-of-interest (ROI) boundaries and re-sampling the image data to a common-sized grid. Landsat-8 satellite OLI-TIRS scenes (but also Sentinel) are recommended, taking into account their resolution and surface reflectance properties. Landsat-8 thus acquires data at the visible and near-infrared (VNIR), short-wave infrared (SWIR) and thermal infrared (TIR) regions of the electromagnetic spectrum. The ground-sampling area breadth of the VNIR and SWIR bands is 30 m², and that of TIR is 100 m².

The second step involves creating training areas (TAs) within ROI. These correspond to polygons of similar and homogeneous LCZs over patches of appropriate dimensions; a square kilometre is considered optimal. The material for processing TAs is obtained from the Google Earth platform, which includes freely-available satellite images of most of the world's cities. LCZs are created as uniform urban designs, but their spectral signatures may differ around the world, within an individual country, or even within a single city. Skill and experience on the part of local experts/researchers is therefore crucial to the creation of TA data if the surface specifics of the city are to be established and the maximum LCZ classification accuracy achieved [52,102].

The third step entails geometrical pre-processing and application of the LCZ classification using open-source SAGA-GIS software. As Bechtel et al. [102] pointed out, LCZ mapping in Landsat scenes is provided by using a random forest (RF) classifier, which is the categorisation algorithm implemented in SAGA-GIS. The classification algorithm recommended for WUDAPT is a RF classifier, consisting of integrated decision trees that allocate each image pixel to one LCZ type [52]. Using the steps above, Bechtel et al. [102] were the first to test the WUDAPT L0 method, for the European cities of Hamburg (Germany) and Dublin (Eire) and obtained a spatial distribution of LCZs (with grid sizes of 100–120 m²) that was well defined and of accurate delineation. A last processing step may involve additional post-classification filtering, in order to obtain a more homogeneous structure of LCZ map should the LCZs prove too fragmented and the map insufficiently legible. This iterative filtering process should be performed as many times as are required to achieve high-quality LCZ maps [52]. Finally, LCZ mapping by means of WUDAPT L0 may deconstruct cities into distinct urban landscapes, based on a range of physical parameters [102], parameters that generate similar thermal signatures at a neighbourhood scale. To date, LCZ classification has been established by the WUDAPT method for many cities in western Europe [102,105–110], in central Europe [102,109,111–119], southern Europe [109,120–122] and eastern Europe [123], as well as throughout Europe [124].

Numerous studies have sought to improve the accuracy of LCZ mapping, most of them proposing upgraded versions of the WUDAPT method or comparing WUDAPT L0 data with other independent urban surface sources. Demuzere et al. [66,125] created LCZ classification maps for urban areas across the European continent and for 15 selected cities around the world, an important step in the further establishment of global urban-surface databases and a major contribution to urban climate studies. They up-scaled the conventional WUDAPT L0 method from a city-by-city approach to a continental scale, maintaining the quality of surface data and the spatial resolution of maps by implementing a combination of TA “transferability” [52] and multi-source data (such as Sentinel 1 and 2, DMSP, and OLS) from Google Earth Engine (GEE) cloud storage. Danylo et al. [123] compared LCZs obtain from the WUDAPT method with the GlobeLand30 and OpenStreetMap (OSM) for cities in Ukraine in order to disclose inconsistencies arising between individual LCZs established via WUDAPT L0 and the situation in the field. Verdonck et al. [105] drew attention to a weakness of the WUDAPT L0 protocol linked to low(er) classification accuracy (particularly for built-up LCZs), and proposed a contextual classifier that included neighbourhood information into the LCZ mapping processes, achieving an improvement in overall accuracy (OA) of 5–13%. OSM data have also been deployed to further enhance the OA of LCZ mapping and refine accuracy for certain classes, among them heavy industry, agricultural land, and water [126]. Implementation of various classifiers, such as convolutional neural networks (CNNs) with multi-source datasets (Sentinel-2, Landsat-8, GUF, OSM, VIIRS-NTL) has been presented in Qui et al. [109]. Further, random forest (RF) with CNN, in Yoo et al. [121], has the capacity to improve the classification for specific LCZs (buildings/trees combinations) and may increase the accuracy of LCZ mapping by up to 30%.

It has been suggested that, in the mapping of LCZs at various scales, the spectral reflectance of Landsat-8, Sentinel-2 and RapidEye may be employed as input features [109,127]. Use of Landsat-8 is quite frequent [102], although a number of authors have

processed data from multi-temporal Sentinel satellite imageries for their LCZ mapping and incorporated this data into a range of models or classifiers to improve built-up height and density in morphological characterisation [128]. This approach has obtained LCZ mapping on a large scale with a higher degree of OA [64,129–131].

Some studies [119,120,122] have demonstrated that LCZ data can improve model performance by incorporating the LCZ scheme generated from WUDAPT L0 into the weather research forecasting (WRF) model, i.e., they have shown that the building effect parameterization-building energy model (BEP-BEM) is sensitive to landscape heterogeneity.

Finally, a few studies [132,133] have focused on comparison of LCZs maps generated from WUDAPT L0 with GIS-based approach data, such as MAppUCE or Vienna GIS, in order to detect general drawbacks or specific LCZ shortcomings/advantages of the remote-sensing classification method. However, Hammerberg et al. [132], maintain that employing GIS-based approaches provides only marginal overall improvements over using the default WUDAPT method. Table 3 summarizes the studies analysed in this section.

Table 3. Remote sensing imagery-based methods for LCZ mapping derived from the studies identified in this review.

Method Used	Study	City/Region Analysed	LCZs Classes Detected
WUDAPT L0 method development	[102] [52]	Hamburg (Germany); Dublin (Eire) Globally, including Europe	All 17 LCZs All 17 LCZs
WUDAPT L0 method	[123]	Kyiv; Lviv (Ukraine)	2, 4, 5, 6, 8, 9, A, B, C, D, E, F, G
	[111]	Szeged (Hungary)	2, 3, 5, 6, 8, 9, A, B, D, G
	[112]	Berlin (Germany)	2, 4, 5, 6, 8, 9, A, B, C, D, F, G
	[113]		
	[105]		
	[106]	Antwerp; Brussels; Ghent (Belgium)	1, 2, 3, 6, 8, 9, 10, A, B, D, E, G
	[107]	Brussels (Belgium)	
	[114]	Augsburg (Germany)	2, 5, 6, 8, A, B, D, F, G
	[118]	Dijon (France)	2, 3, 4, 5, 6, 7, 8, 9, 10, A, B, C, D, E, G
	[108]	Globally, including Europe	All 17 LCZs
	[65]	Budapest (Hungary)	2, 5, 6, 8, A, D, G
	[116]	Szeged (Hungary); Novi Sad (Serbia)	2, 3, 5, 6, 8, 9, 10, A, B, C, D, E, F, G
[117]	Amsterdam (The Netherlands)	All 17 LCZs	
[110]	Globally, including Europe	All 17 LCZs	
[124]			
WUDAPT L0 + OSM	[126]	Hamburg (Germany)	1, 2, 4, 5, 6, 8, 10, A, B, D, G
WUDAPT L0 + EE	[66]	European continent	All 17 LCZs
	[125]	Globally, including Europe	All 17 LCZs
WUDAPT + CNN	[109]	Amsterdam (The Netherlands); Zurich (Switzerland); Rome (Italy); Paris (France); Munich (Germany); Milan (Italy); London (UK); Cologne; Berlin (Germany)	All 17 LCZs (except LCZ 7)
WUDAPT + CNN/RF	[121]	Rome (Italy); Madrid (Spain)	2, 3, 4, 5, 6, 8, 9, 10; A, B, C, D, E, F, G
WUDAPT to WRF	[120]	Madrid (Spain)	1–10
	[119]	Vienna (Austria)	2, 6, D _E
	[122]	Bologna (Italy)	2, 5, 6, 8, A, B, D, E, G
Sentinel-2 + TDM	[128]	Germany, The Netherlands; UK cities	Nine density/height classes based on LCZ concept
Sentinel-2 + Re-ResNet	[129]	Amsterdam (The Netherlands); Paris (France); Munich (Germany); Milan (Italy); London (UK); Cologne; Berlin (Germany)	All 17 LCZs (except LCZ 7)
Sentinel-2 + CNN	[130]	German cities	1, 2, 4, 5, 6, 8, 9, 10, A, B, C, D, E, F, G
Sentinel-1	[64]	Globally, including Europe	All 17 LCZs

Table 3. *Cont.*

GEE	[131]	Oslo (Norway)	2, 3, 4, 5, 6, 8, 9, A, B, D, E
RF	[127]	Milan (Italy)	2, 3, 5, 6, 8, B, D, G
WUDAPT/MApUCE	[133]	Paris; Toulouse; Nantes (France)	All 17 LCZs
WUDAPT/Vienna GIS	[132]	Vienna	All 17 LCZs
WUDAPT/GIS method (Geletič and Lehnert 2016)	[115]	Bratislava (Slovak Republic); Brno (Czech Republic); Kraków (Poland); Szeged (Hungary); Vienna (Austria)	All 17 LCZs

3.2.4. Combined Method

The methods of LCZ detection and mapping considered as “combined” are usually characterised as various blends of approach, datasets and tools (Table 4), but they also employ calculations involving integrated surface parameters and other properties defined by Stewart and Oke [33]. Reasons for using combined methods include overcoming any lack of detailed surface morphological/and cover data, presentation of alternative approaches that provide comparisons with GIS-based methods [51], and improvement of the calculation sensitivity of remote sensing-based methods [102].

Table 4. Combined methods for LCZ mapping derived from studies identified in this review.

Method(s) Used	Study	City/Region Analysed	LCZ Classes Detected
LULC + GE/BM	[134] [135]	Dublin (Eire)	2, 3, 5, 6, 8, 9, 10, A, D, E, F, G
LULC + MOLAND	[136]	Dublin (Eire)	2, 3, 5, 6, 8, 9, 10, A, D, E, F, G
LULC + GIS/models	[137] [138]	Basel (Switzerland)	2, 2 ₃ , 2 ₁₀ , 2 _A , 3, 5 _E , 6, 9, 10, 10 ₂ , A, A _E , C, D, D ₉ , E ₁₀ , G, G _A
WRF-SLUCM-LCZ model	[139]	Szeged (Hungary)	2, 3, 5, 6, 8, 9, D, G
OSM + UA + field work	[140]	Augsburg (Germany)	2, 5, 6, 8, A, B, D
Admin. data + SOLWEIG	[141]	Berlin (Germany)	5, 6, A, B
OS + LiDAR	[49]	Glasgow (Scotland)	2, 5, 6, 9
Admin. data + LiDAR	[142]	Glasgow (Scotland)	LCZ 2
WUDAPT + field work	[143]	Berlin (Germany)	2 _B
Admin. data + UA	[144] [145]	Birmingham (UK)	1, 2, 5, 6, 10, B
MAES model + GIS	[63]	Bulgarian cities	All 17 LCZs (except LCZ 1)
Multi-admin. data	[62]	French cities	1, 2, 3, 4, 5, 6, 7, 8, 9, D, E, G
GIS + DSM	[146] [147] [148]	Nancy (France)	2, 5, 8, 6/9, A, B, D, E, G
SURY model + WUDAPT	[149]	Belgian cities	All 17 LCZs
Field work + WUDAPT	[150]	Hamburg (Germany)	2, 4, 5, 6, 8, 10, A, B, D, E, G
GIS + field work	[151]	Braganca (Portugal)	2, 3, 5, 8, 9, A/B, C/D

Conversion of land-use land cover (LULC) datasets obtained from global or regional sources into LCZ classes is a further approach to mapping LCZs. Dublin (Eire) has been successfully LCZ-mapped at a resolution of 1 km² by “translating” morphological data from the LULC CORINE dataset (developed by the European Environmental Agency) into LCZ classes by means of freely-available web-based tools such as Google Earth (GE) and BingMaps (BM) [134,135] and application of the MOLAND model [136]. Wicki and Parlow [137] and Wicki et al. [138] defined the LCZs for Basel, Switzerland, by obtaining the

LULC types from the Landsat-8 dataset, and then applying calculations of morphological parameters with GIS tools and models (UMEP and DSM), based on the city's administrative data, in order to convert LULC types to LCZs. Molnár et al. [139] created a WRF-SLUCM-LCZ modelling scheme to synthesise canopy parameters and harmonize LULC data with LCZs, then assigned LCZ classes to the urban grids of WRF. Straub et al. [140] combined open-source data for surface characteristics (Open Street Map and European Urban Atlas), wide-angle photographs from field work and a digital terrain model from the Bavarian State Office for Survey and Geoinformation, in order to calculate LCZ classes around the HOBO logger station locations in Germany.

The use of land-cover information from national or local (city) administrations and combining these datasets with other surface measurements (e.g., remote sensing, GIS data, field work) is interesting. Fenner et al. [141] obtained land-use characteristics from the Berlin Senate Department for Urban Development and the Environment and used the SOLWEIG model (for sky-view factor calculations) and field work to determine the LCZs within a radius of 500 m around each UMN (urban meteorological network) station. Both Emmanuel and Loconsole [49] and Maharroof et al. [142] used the Ordnance Survey maps, representing the UK's national land-cover information, and the City Development Plan of Glasgow, respectively, and LiDAR data for estimation of building cover, building height and LULC, and also applied Google Earth and field work for the verification process. LCZ mapping of a specific study area in Berlin, based on a combination of the approach taken by Fenner et al. [112] and calculations of geometric parameters from field work (using wide-angle photographic data), has provided surface feature outcomes at the micro-scale level [143]. Furthermore, Bassett et al. [144] and Feng et al. [145] used urban surface information from the Birmingham region's administrative authority (UK) and from the Urban Atlas land-use types classified by the European Environmental Agency, to detect LCZs classes around BUCL (Birmingham urban climate laboratory) station locations. Nedkov et al. [63] employed the three-level MAES (mapping and assessment of ecosystems and their services) typology, where the third level included LCZ classes that contributed to more detailed spatial representation of the study area by applying GIS-based analyses and visual interpretation of orthophoto images. Using the combination of building and surface databases from France's national administration sources, such as the MApUCE project, BD TOPO, GENIUS, and INSEE, Gardes et al. [62] obtained detailed object and land-cover features in order to calculate the LCZ patterns of French cities.

Urban surface calculations that apply a combination of surface data and GIS-based or remote sensing-based concepts appear in a number of studies. In the LCZ mapping of the Nancy (France) urban area, the surface metadata gathered from field work and remote sensing sources were worked up by means of GIS tools (SAGA GIS), models (DSM) and manual calculations to obtain SVF, terrain roughness (Davenport calculations), building heights (from the national database of building footprints), ISF/PSF, and more [146–148]. A combination of models, such as SURY v1.0 (semi-empirical urban canopy parameterization), implemented in COSMO(-CLM) [149] or using topographic/aerial images [150] with the WUDAPT urban database platform, may produce high-resolution LCZ mapping. Goncalves et al. [151] combined a GIS-based approach with field work (wide-angle photographs) for LCZ mapping in Portugal.

3.3. Thermal Analyses Using the LCZ Concept

The seminal Stewart and Oke [33] study indicates that LCZ classification provides urban surface metadata for UMN station locations in built-up and land-cover zones. This facilitates further heat load assessments among the various urbanization types. This classification method has also proven to be a promising approach when researching the intensity and spatial distribution of temperatures, UHI, and other thermal and climate risk indices. Consequently, some 75% of the studies analysed (except those addressing methodology or station site metadata) have focused on heat load analysis. More specifically, Figure 9 shows the proportions of studies based on the types of datasets and analysis that have employed

the LCZ concept. Sections 3.3.1–3.3.4 below present outcomes of the studies reviewed. These have been kept brief in order to facilitate legibility; any other approach would overload the review with numerical detail, obscuring the main points. Thus, these subsections provide the essence of the analysis or the results for each study, while additional details appear in Supplementary Materials Table S1. Should more in-depth information be required for any given study, it may be found directly through the DOI link presented in Supplementary Materials Table S2.

Further, Supplementary Materials Table S1 presents thermal patterns based on the LCZ scheme as applied to several European cities. These have been divided into night-time (after sundown) and daytime (after sunrise) periods. The majority of studies cover the night hours, since stronger and clearer signals of thermal differences between LCZs, as well as between built-up and land-cover LCZs, occur during this period. A division based on the type of dataset has also been made, separating thermal analyses from fixed, mobile and remote sensing measurements, or by modelling approaches. In Supplementary Materials Table S1, for each selected city, we present: (a) the source of the dataset, expressed as the number of stations or satellite scenes and time period of analysis; (b) the (bio)meteorological/climatological characteristics such as air temperature, surface temperature, outdoor thermal comfort indices, etc.; (c) references to studies in which more details appear; and (d) most importantly, the order of LCZs according to reported characteristic(s), e.g., how temperatures differ in terms of LCZ class (see Section 3.3.5).

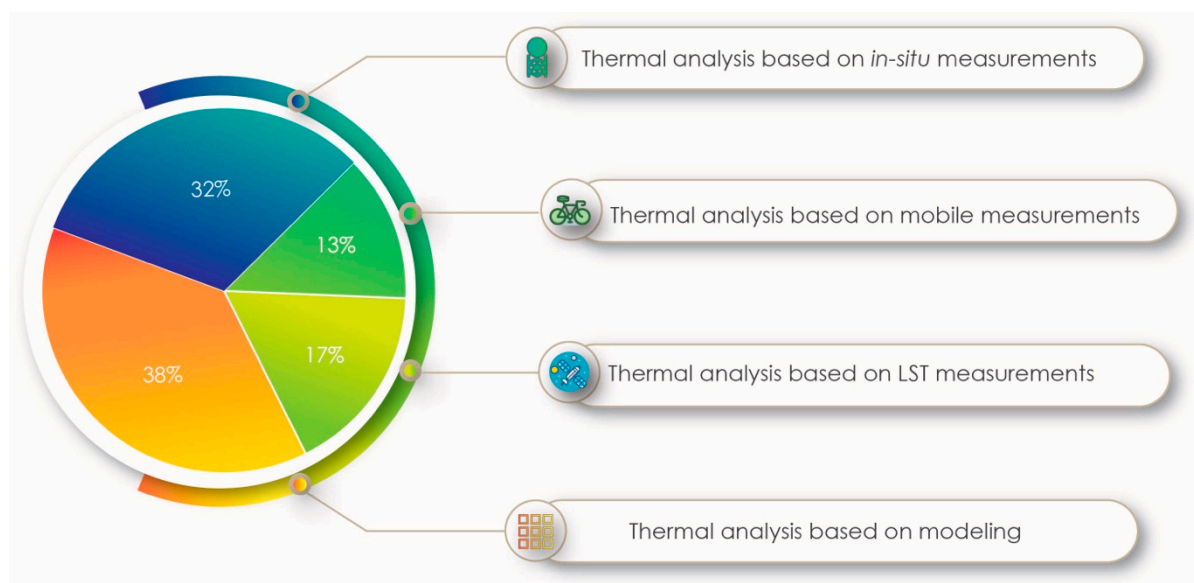


Figure 9. Distribution of the studies reviewed, arranged by type of dataset/analysis used for the thermal patterns of LCZs. Note: Only the articles focusing on thermal analysis are included in the chart (66 studies in total).

3.3.1. Thermal Analysis Based on In-Situ Measurements

In a number of studies, the spatial patterns of air temperatures or other meteorological values obtained from UMNs are investigated and presented as differences between LCZs. Studies that analysed seasonality or day/night variability of temperatures and related indices within urban areas, as well as spatiotemporal assessments of UHI intensity after sunset, are particularly interesting [86,89,114,127,134,150]. Intra-urban temperature or outdoor thermal comfort observations are also worthy of note [26,85,90,91]. Further, Gonçalves et al. [151] assessed UHI and UCI (urban cool island) characteristics in the LCZs of a small city in Portugal. Fenner et al. [141] used long-term datasets to present air temperature differences between built-up LCZs and LCZ B, with particular attention to night-time and summer, while Quanz et al. [143] focused on thermal assessment of the LCZ 2_B class, using eleven stationary T_a sensors. Fenner et al. [112] used CWS (citizens

weather station) datasets to address intra-/inter-urban air temperature variability among LCZs and later to analyse UHI intensities [113]. In the urban area of Birmingham (UK), Feng et al. [145] employed a combination of UMN BUCL (Birmingham Urban Climate Laboratory) and MODIS scenes to analyse UHI and SUHI patterns based on the LCZs. Assessments of outdoor thermal comfort (OTC) show that densely built-up LCZs (such as mid-rises and large low-rise zones) have considerable impacts on thermal conditions in terms of higher/discomfort PET or UTCI values [74,85,87]. Savić et al. [92] assessed and mapped heat-wave risk zones using the night-time temperatures from UMN NSUNET (Novi Sad urban network, Serbia) system and the general LCZ pattern of the city. Wiesner et al. [73], investigated relations between air temperature anomalies and soil moisture, but differences in mean annual T_a among urban/non-urban LCZs were about 1 °C (day-time) and 1.7 °C (night-time), clear evidence that topsoil moisture effects on UHI were not evident.

3.3.2. Thermal Analysis Based on Mobile Measurements

Deriving their conclusions from mobile measurements, Stewart et al. [50] presented differences in the magnitudes of air temperature within the framework of LCZs. Several studies have used mobile measurements to detect T_a patterns among built-up and land-cover LCZs, additionally coordinating their measurement campaigns with daytime and night-time periods of the day [97,142,146–148], or with particular seasonal/extreme weather periods (e.g., summer season or heat-wave period) [75,96]. The results indicated distinct temperature differences between LCZs, with a tendency towards decreases towards the outskirts. Rathmann et al. [118], using mobile measurements through built-up and land-cover LCZs posited that LCZs in which there is a predomination of urban forest/urban greenery ameliorate subjective OTC and contribute to human well-being. Such studies, however, were frequently deliberately designed to point out to and quantify intra-zonal air temperature variability between LCZs.

3.3.3. Thermal Analysis Based on Land-Surface Measurements

Geletič et al. [95] derived LSTs from the two satellites, LANDSAT-8 and Terra ASTER, and explored the extent to which LCZ classes discriminate in terms of LSTs in Brno and Prague (Czech Republic). Later, Geletič et al. [93] used LST data derived from LANDSAT-8 for Brno, Prague and Novi Sad (Serbia) and assessed the inter/intra-zonal seasonal variability of SUHIs in various LCZs. An interesting element arose out of this: the definition of additional eleven land-cover subclasses to facilitate more detailed LST analysis of land-cover LCZs. Gémes et al. [88] used LANDSAT-4, 5, 7, and 8 databases (from 1984 to 2016) to perform an analysis of LST and SUHI seasonality in the LCZs of Szeged (Hungary), while Oliveira et al. [100] analysed correlations between LSTs and LCZs in five southern European cities, Bechtel et al. [65] performed a similar LST analysis for the whole world (including Europe). Fricke et al. [117] addressed intra-/inter-urban SUHI patterns based on LCZs, using the MODIS datasets for Szeged (Hungary) and Novi Sad (Serbia), while Dian et al. [116] did the same for the city of Budapest (Hungary). Gholami and Beck [124] determined the relationship between LST and LCZ for 25 cities worldwide, but with only a few examples for European cities. Pour et al. [76] and Pour and Voženílek [77] took airborne thermal images (using a thermal camera installed in a light aeroplane) for the city of Olomouc (Czech Republic), and determined that the highest surface temperatures occurred in LCZs 2, 4, 5, and 8. In similar fashion, Skarbit et al. [84] analysed LST differences between the LCZs of Szeged on the basis of airborne thermal measurements during the early night hours, and the general results indicated that LCZ 6 has the lowest early night-time LST compared with other densely built-up LCZs such as LCZs 2, 3, and 5.

3.3.4. Thermal Analysis Based on Modelling Approaches

Prediction of air temperature, OTC and other climate indices at local scales would constitute significant progress in urban climate research. In this light, a number of studies

have compared modelled and simulated data with measured datasets, using numerical model MUKLIMO_3 [5,94,98,111,115] or other numerical models, such as WRF [119,139]. Brousse et al. [120] modelled the spatial temperature characteristics of LCZs using the WRF model and McRae et al. [152] included LCZs in a WRF simulation of boundary conditions for ENVI-met, using San Jose (California) as an example town. Richard et al. [108] addressed the relevance of LCZs and UCZs to temperature patterns by using measured T_a , but also modelled temperatures (using WRF). Satellite and crowd-sourced temperature datasets at very fine resolution were combined in the urban part of Oslo (Norway) then LiDAR and terrain data within an RF regression modelling framework were built in to map temperature patterns [131]. The results demonstrated that this method is broadly transferable to cities with private weather station data. Theeuwes et al. [78], using of the BUBBLE campaign dataset, presented magnitudes from modelling UCI for nine built-up LCZs (not LCZ 10) and obtained maximum UCI ranges from 1.6 °C (LCZ 7) to 3.2 °C (LCZ 4). Basset et al. [144] used 29 UMN weather stations in Birmingham (UK) for a spatial interpolation of UHI and observed a UHI advection process in the urban area, while Wicki et al. [138] modelled and evaluated UHI intensity within the LCZs of Basel (Switzerland), also using UMN datasets. Straub et al. [140] employed a statistical modelling approach to the assessment of spatial patterns of UHI intensity, while Gardes et al. [62] focused on the night-time UHI intensity in French cities in terms of urban morphology parameters. Emmanuel and Loconsole [49] introduced a low data-intensity and easy-to-use method for classifying urban areas into LCZs, and made an assessment of the performance of green infrastructure in the mitigation of urban overheating in various LCZs of the Clyde Valley, Glasgow, Scotland. They employed air temperatures (measured at a GCU station) and those simulated in ENVI-met, confirming that green infrastructure could well be important in alleviating urban overheating in future warmer conditions. Alexander et al. [135] deployed the SUEWS simulation model, using meteorological data from a station outside Dublin city centre (Eire) and a detailed description of urban surface features (based on the LCZ concept) to establish urban energy balance conditions. Alexander et al. [136] used simulation models to evaluate future urban development scenarios and their impact. Their results suggested that the optimal development scenario includes the preservation of a higher proportion of vegetated land-cover areas. Wouters et al. [149], basing their work on modelled surface and air temperatures for Belgian cities with the COSMO-CLM atmospheric numerical model, concluded that the implementation of SURY canopy parameterization, the WUDAPT concept, and advances in atmospheric modelling systems for further urban climate research, are vital. Verdonck et al. [107] analysed the GHG scenario in combination with LCZ classes to project heat stress for the year 2090; their results indicate an increasing tendency in every LCZ class in comparison with present-day climate conditions. Tornay et al. [60] employed the GENIUS database structures and TEB model simulations to determine the sensitivity of the urban surface energy balance to building architecture and contributed to the definition of urban typology and buildings for further urban climate research. Droste et al. [79,110] simulated urban wind-island effects and investigated wind-speed distribution in various LCZs. The results of Hammerberg et al. [132], from a study employing measured temperature datasets from CWS/official stations and modelled data for comparison of seasonal differences in LCZs defined by WUDAPT and Vienna GIS methods, are especially interesting.

3.3.5. Summary of Thermal Responses of Local Climate Zones

Overall results suggest that the highest temperatures occur in densely built-up LCZs, such as LCZ 2, LCZ 3, and LCZ 5, and also in cities in which LCZ 1 has been detected. Furthermore, higher temperatures, such as those in LCZs 1–5 are evident in cities where industrial zones, such as LCZ 8 and LCZ 10, are sharply defined, an obvious consequence of densely-built surfaces and a high proportion of ISF characteristics. In nearly all cases, towards the outskirts (i.e., LCZ 6 and LCZ 9), the temperature decreases, and the lowest values occur in land-cover LCZs, such as LCZ A, LCZ B, and LCZ D.

Examining in more depth the outcomes of night-time heat load patterns within LCZs, based on both air temperature datasets (mobile or in-situ) and LST datasets, it becomes evident that: (a) heat load patterns for LCZs in mid-sized cities (the analysis undertaken in the majority of cases), as well as for large cities (such as Brussels, Berlin, etc.) are similar; (b) these heat load patterns remain similar during the summer periods as well as in the winter periods; and (c) heat load are tending to increase from land cover/low densely-built types towards densely built LCZs, such as LCZs 1, 2, 3, and 5 (Supplementary Materials Table S1). A few studies may serve as examples. The mean annual T_a difference (based on the decadal period 2001–2010) between LCZs 5 and B in urban areas of Berlin occurred at a value of 6 K during the summer night-time period [140]. Leconte et al. [146,147] and Lehnert et al. [96,97], using mobile temperature measurements, determined average night-time air temperature differences between pairs of LCZs that varied from less than 1 °C for close LCZs (LCZ 6/9-LCZ D) to more than 4 °C for dissimilar LCZs (LCZ 2-LCZ D, LCZ 5-LCZ D). Analysis of the PET differences for Novi Sad (Serbia) in the night-time revealed that, during a heat-wave event, the maximum occurred between LCZ 2 and LCZ D at a value of over 7 °C and almost 5 °C between LCZ 5 and LCZ D [87], while the highest nocturnal differences detected by Unger et al. [90] in Szeged (Hungary) reached a value of 6 °C between LCZ 2 and D.

Detailed analysis of daytime heat load patterns in terms of LCZs, also using various types of measured datasets, shows: (a) lower thermal differences (comparing to night-time) in a range of urbanization types in mid-sized and large cities; (b) these heat load pattern tendencies are similar at various periods of the year; (c) thermal outcomes are at their highest values in the most densely-built LCZs types (LCZs 2, 3 or 5), but often happen during the daytime to occur in LCZs 8 or 10 (Supplementary Materials Table S1); and (d) compared with the night-time heat load differences between LCZs, differences in values are lower during the daytime [87,90,97]. For instance, Fenner et al. [141] pointed out the complexity of differences between LCZ 5 and B during the daytime, since at certain parts of the day (morning or afternoon) the LCZ 5–LCZ B difference is negative, while it is positive at midday. Furthermore, this analysis revealed that, in some cases, differences between LCZ 5 and B were higher than 10 °C (taking daytime and night-time into account). Geletič et al. [95], addressing LST for Prague and Brno (Czech Republic), disclosed the highest temperature values for LCZ 10, with differences that could reach around 15 °C (LCZ 10–LCZ A). These results were based on weather conditions for days upon which the satellite scene could be presented. LCZs 3 and 2 exhibit high heat loads and differences between them and LCZs A or G may range from 10 to 15 °C. Unger et al. [90] analyzed PET differences in Szeged (Hungary) during the summer period and disclosed that the highest value differences occurred between LCZs 2 and D in the afternoon (3.6 °C) and evening periods (3.5 °C). Furthermore, during a particular heat-wave period (12–16 August 2015, Szeged) the highest PET differences achieved 2.6 °C (LCZ 2–LCZ D), and intra-urban differences were lower: on the whole, under 2 °C. Müller et al. [74] presented the diurnal variation of PET within the LCZs of the urban area of Oberhausen (Germany) on 10 July 2010 and the highest differences occurred between LCZs 2 /5 and LCZ 9, ranging from 5 to 10 °C, while intra-urban differences reached 1–2 °C (e.g., LCZ 2–LCZ 6 and LCZ 6–LCZ D).

A general summary could posit that night-time temperature patterns within LCZs are more dependent on dense urbanization and building heights when compared with daytime LCZ thermal patterns. Turning to night-time values, a clear decreasing tendency of heat load from LCZs 1, 2, 5, or 3, towards LCZs 8, 10, 6, 9, or land cover types, is evident. Obviously, those with densely built-up characteristics, buildings mostly higher than three storeys (such as in LCZs 1, 2 and 5) slow down the emission/release of heat accumulated during the daytime when the sun was above the horizon, with the result that higher near-surface temperatures persist all night. In other respects, thermal distributions in terms of LCZs during the day-time are not as uniform as during the night, i.e., according to the data, the warmest LCZs are, apart from LCZs 1, 2, and 5, LCZs 10, 8, or 6 as well. These situations arise because urban areas with densely-built and higher buildings cast more

shadows during the daytime and the heat load accumulation process is slower compared with that in LCZs 8 or 10, where most of the buildings are lower than three storeys and not so dense (fewer shadows). However, the proportion of ISF must still be considered.

A substantial contribution to intra-zonal temperature differences, and their impacts, in built-up areas may well be made by the relative amount of vertically-oriented surfaces, expressed in terms of building height or width proportions, and also by surface insolation changes with the seasons. These factors were largely responsible for the sharp differences between built-up LCZs and land-cover LCZs, particularly when LST datasets were examined by Geletič et al. [93]. Differences in building materials, urban characteristics, the size of the urban space and its topography and local/regional climate could also contribute to different LCZ thermal patterns, as Geletič et al. [93] discussed, contrasting the examples of Prague and Brno (Czech Republic) and Novi Sad (Serbia). The urban area of Novi Sad is smaller than that of Prague or Brno, and certain LCZs, such as 4, 5, 6, and 9, are scattered and non-homogeneous. Further, the relatively higher heat load, particularly LST, in LCZ D of Novi Sad, resulting in several insignificant LST differences with other LCZs in winter, spring and autumn (mostly in early spring and late autumn), i.e., during non-vegetation periods, is explainable there by the local specific of particularly dark soil of low albedo. Furthermore, the influence of topography, especially in forested areas in high mountains, on the near-surface temperature patterns, and also LSTs [153], cannot be ignored, especially when the properties of the tops of tree crowns are taken into consideration.

4. Challenges and Further Development

Stewart and Oke [33] developed the LCZ classification system to enhance standardization in urban climate research. However, it was created as a robust system, featuring a reasonable number of built-up and land-cover classes, in order to be applicable at a global level. Nevertheless, certain studies have discussed additional subclasses in urban [25] and non-urban [93,119] zones, on the grounds of obtaining more detailed and clearer spatial thermal signals. Such a subclass approach is probably difficult to implement widely, and Alexander and Mills [134] have concluded that it is rather necessary to standardise the method for detection and delineation of LCZs in urban areas in a uniform way that can be sufficiently applied throughout the world.

It may be anticipated that particularly methods for urban surface classification, based on open-sources and global data, will have the capacity for broad application and constant development. This makes good sense, especially if it is user-friendly, i.e., does not demand high skills in modelling, the use of GIS tools, or imagery processing. To date, the WUDAPT method has emerged as an approach that might fulfil these conditions. It was developed as an international community portal to gather surface information concerning urban areas at a global level and to facilitate further urban climate research [103]. As result of this global initiative, WUDAPT L0 data are currently available for more than 120 cities across all continents (available at: <http://www.wudapt.org/outreach/papers/> [101], accessed on 15 December 2020). Currently, based on the analysis of the European studies performed herein, as well as a number of contributions beyond the European region [52,103], the WUDAPT method stands out as a solution for LCZ mapping; many researchers consider it standard for the delineation of LCZs. However, in view of the peculiarities of this method, and further development and improvement (which we leave to others), the desired level of standardization in urban climate research may remain a matter for discussion. Ching et al. [103] and Bechtel et al. [52] have addressed the implementation of measures to overcome the shortcomings of LCZ mapping by the WUDAPT L0 method, and have highlighted possible approaches to the quality assessment processes. Although several different approaches to LCZ mapping using remote sensing data have been presented (see Section 3.2.3), researchers have reserved their closest attention for further development and verification of the overall accuracy (OA) of the WUDAPT method. In general, possible steps and improvements for the further use of remote sensing methods in LCZ mapping may be classified as:

- Higher accuracy in defining training areas (TAs). With the aim of standardizing the LCZ classification process, the most problematic, even controversial, step is the highly subjective (expert-based) selection of TAs, particularly in cases where the classification for each urban area must be trained individually [66]. Hence, LCZ mapping might prove quite complicated. Similar LCZs in different regions have dissimilar spectral properties due to differences in vegetation, building materials and other variations in cultural and physical environmental factors [102]. Outcomes appear to indicate that LCZ maps are of only moderate quality, i.e., around 50–60% in terms of OA, and some studies have demonstrated that appropriate selection of TAs may increase OA by around 20–30% [66]. However, the quality of TAs remains the foundation of the protocol for generating LCZ maps [103]. Working on standardization of perspectives in defining the typical built-up zone/LCZ, and enhancing the expertise of the volunteer local experts/researchers involved in classification of satellite images, may be a crucial move towards defining TAs with higher accuracy for cities around the world. In this light, Bechtel et al. [154] pointed out that results from the Human Influence Experiment (HUMINEX) revealed large differences between LCZ maps for a single city as developed by different researchers. The HUMINEX outcome suggested that a high-quality LCZ map for a given city can be achieved by the use of ten to fifteen individual TA sets created by untrained experts/researchers. However, this proposal appears in need of further investigation.
- Better quality of satellite images. Current possibilities for the improvement of the accuracy of LCZ mapping include the combination of moderate-resolution satellite images and encouraging researchers to employ other data sets in parallel [52]. Dian et al. [116] presented a series of satellite images from geostationary satellites together with their advantages and disadvantages for use in spatial and climate analysis. It follows that very high-resolution aerial imagery obtained from commercial satellites and unmanned aerial vehicles (UAVs) should be beneficial to accurate LCZ mapping. However, these remain to be studied in detail and data sets are not yet freely available.
- Quality assessment approaches. Bechtel et al. [52] contributed a detailed discussion of the importance of WUDAPT L0 method to the quality assessment and of the checking steps required for successful LCZ maps. They drew attention to an automated cross-validation approach that applies bootstrapping measures [155,156], followed by manual review [52], in a way that involves human visual comparison of the map with high-resolution imagery from Google Earth, and a cross-comparison approach whereby LCZ maps may be compared with other independent data-sets. These cross-comparisons between WUDAPT L0 LCZ maps may be performed in parallel with many sources, among them: GHSL-LABEL (global human settlement layer) or the EEA (European Environment Agency) soil-sealing data set [156]; with selected city-specific comparisons; together with Geo-Wiki data [157]; Google Street View imagery [158,159]; Google Street Map [160]; with vector datasets developed by the nationally-funded MApUCE project [133]; by comparison with the GIS-based method [51]; or by comparisons based on air temperature measurements [114]. Hence, the cross-comparison approach has the potential to become an obligatory step in the standard evaluation procedure for further research [52].
- Improvements in the methods of LCZ mapping. There exist various ongoing suggestions for improvements to the methods of producing LCZ maps and refining their accuracy. Kaloustian et al. [161] recommended transferability of TAs from one city to another. Tuia et al. [162] proposed the development of a robust, generalized classification model. Xu et al. [160], while analysing the Hong Kong urban area, proposed a co-training-based approach, without the need for TAs, and obtained 10% more OA compared with conventional approaches. Using online processing platforms that contain a range of Earth observations could help improve LCZ mapping, and Google Earth Engine has been of value in a number of studies [66,125,163]. It may be concluded that implementation of deep-learning technologies could contribute

to extracting high-level image features in order to improve classification accuracy, and this issue will certainly be the focus of further studies [52].

- Application in urban climate modelling. LCZ mapping data is considered a useful input parameter (urban canopy parameter–UCP) for the urban modelling process, so the WUDAPT method could potentially contribute to urban climate models. Hammeberg et al. [132] highlighted that WUDAPT L0 data has advantages in providing the necessary surface parameters for urban climate models and assists the intra-urban classification of surface characteristics and thermal analysis. Thus, the first studies demonstrated that clear signals of surface heterogeneity may be obtained from LCZ mapping, using the WRF model [120,132]. Also, Ching et al. [103] drew attention to portal tools such as WUDAPT to WRF (W2W) and SCALER as having great potential for future research. However, in the light of the studies analysed herein, there still exist uncertainties about the utility of LCZs for fine-scale modelling in urban areas.

Although other LCZ mapping methods, such as GIS-based or combined, provide adequate accuracy for defined urban and land-cover features, there is not much evidence of capacities adequate for the classifications of large-scale areas, i.e., for covering numerous cities across the continent or the whole world. The reason could be that these kinds of LCZ method require a solid grounding in the use of GIS tools and surface assessments in general. Furthermore, some input parameters for surface calculations are at high resolution scales (e.g., single building footprints) in order to perform LCZ classification at lot area polygon level [51]. Only a few of these kinds of dataset are open-sourced, and are available for only limited urban areas, which may constitute a serious obstacle to the global application of LCZ assessments. According to the high accuracy approach, GIS-based methods, however, could have a certain role in local scale classification and modelling.

Based on the studies reviewed, the vast majority of research has focused on different approaches to thermal assessment, such as air temperatures, surface temperatures, UHI intensities, UCI patterns, thermal comfort issues, heat risk estimation, etc. The predominance of thermal analysis is only to be expected in the light of the proof [33] that specific surface morphology and land-cover types play a significant role in temperature signals and that therefore each LCZ creates a distinct thermal footprint. Other parameters, such as urban wind effects [79,110] or building energy-consumption simulations [60] and biometeorological indices [5,85,87,90,91], have also been investigated. In contrast, spatial pattern assessments of precipitation [164,165] and air humidity [166] have defined a certain quantity of differences between urban and non-urban areas, but do not show clearly distinct values for the different urban areas based on the LCZ concept. Turning to sources of datasets for urban climate assessments, it is noticeable (from 2015 to the present) that remote sensing measurement studies are burgeoning in comparison to measurements in-situ or mobile campaigns. However, despite this trend in datasets, other approaches have much to contribute to further thermal assessments based on LCZs and ways in which temperatures and other climate values are monitored. These include: (a) crowd-sourcing techniques using CWS (citizen weather station), smart-phone records and web-based tools [112,113,131], or (b) using purpose-designed mobile/portable instruments [167] with specifically-numbered and high-accuracy sensors, particularly for radiation measurements [168]. It is clear that, in future research, datasets from LCZ mapping will be frequently present as an input for climate modelling, e.g., WRF [119,120,122] or MUKLIMO [5,53,94,98,111,115]. However, for all their relevance at local scales, LCZs cannot be, or should not be, used for fine-scale models at a higher resolution (e.g., PALM-4U).

5. Conclusions

This review paper gathered and analysed 91 studies that directly address LCZ detection and delineation issues and their application in European urban environments. To date, LCZ classification has proved a universally applicable method of description of the physical environment for the purposes of urban climate research. Over the past eight years, its presence in urban climate research has expanded constantly, particularly in heat

load analyses. A summary of the latter already leads to the conclusion that the highest temperatures in European cities, (or, more generally, heat load patterns) are present in LCZ 1 (where detected), followed by LCZs 2, 3, and 5, then LCZs 8 and 10 in cities with large industrial/commercial zones. Going into the details of thermal outcomes in review studies in terms of annual/seasonal averaged data, the higher temperatures or OTC index values range between 1 and 3 °C between densely built-up LCZs and land-cover zones, but more research on OTC and resulting heat stress in LCZs is required. In the analysis of extreme events (such as heat/cold waves), built vs. land cover types LCZ differences can reach 7–10 °C, or even more. However, the spatial heterogeneity of European environments often renders it difficult to obtain a signal (source area) that is representative of particular zones at a local scale. Researchers therefore frequently face a dilemma as to which zone the area/site should be assigned, and how to indicate sub-classes. This emphasizes the need for a more standardised, universal, and clearly- described LCZ classification procedure. The main necessity for expansion of the LCZ classification system may be found in current absence of internationally consistent urban datasets to represent the parameters of homogenized surfaces. Obviously enough, the global-to-urban climate science communities are aware these issues and recognise them as significant impediments to scientific progress.

Data derived from LCZ mapping and the results of climate analysis based on LCZ patterns may provide sufficient detail to engage local or regional administrative decision-makers charged with addressing climate change issues, urban development and public health [169]. Such applications of LCZs in urban environments play an increasingly important role globally, a fact reinforced by the World Meteorological Organization (WMO), which is exploring the use of LCZ classification methods as a means towards addressing its new urban services mandates, as expressed in Resolution 68 and in the development of the Guide for Integrated Urban Hydrometeorological, Climate, and Environmental Services [170].

Supplementary Materials: The following are available online at <https://www.mdpi.com/article/10.3390/ijgi10040260/s1>, Figure S1: The most prolific sources of LCZ-related articles and the citation connections between them from Scopus (B1) and WoS (B2); and the most-cited sources of LCZ-related articles and citation connections in Scopus (C1) and WoS (C2); Table S1: A brief presentation of temperature changes within LCZ patterns from studies identified in the review; Table S2: The list of 91 reviewed studies related to LCZs issues and with their content details.

Author Contributions: Conceptualization: Michal Lehnert and Stevan Savić; Methodology: Michal Lehnert and Jelena Dunjić (Section 2); Investigation of reviewed studies: Michal Lehnert, Stevan Savić, Dragan Milošević and Jelena Dunjić; Writing—original draft preparation: Michal Lehnert and Stevan Savić (Section 1), Michal Lehnert, Stevan Savić, Dragan Milošević, Jelena Dunjić and Jan Geletič (Section 3), Stevan Savić (Section 4), Michal Lehnert and Stevan Savić (Section 5); Writing—review and editing: Michal Lehnert and Stevan Savić; Visualization: Jelena Dunjić. All authors have read and agreed to the published version of the manuscript.

Funding: This research was funded by internal grant from Palacký University, Olomouc ref. IGA_PrF_2020_029 Spatial analysis of selected environmental and social issues in urban and suburban areas.

Institutional Review Board Statement: Not applicable.

Informed Consent Statement: Not applicable.

Data Availability Statement: Not applicable.

Acknowledgments: This research was supported by an internal grant from Palacký University, Olomouc, ref. IGA_PrF_2020_029 “Spatial analysis of selected environmental and social issues in urban and suburban areas”. Also, the authors acknowledge partial financial support from the Ministry of Education, Science and Technological Development of the Republic of Serbia (Grant No. 451-03-9/2021-14/200125). We would like to extend our thanks to Tony Long (Carsphairn, Scotland) for helping edit the English.

Conflicts of Interest: The authors declare no conflict of interest.

References

- Kovats, R.S.; Valentini, R.; Bouwer, L.M.; Georgopoulou, E.; Jacob, D.; Martin, E.; Rounsevell, M.; Soussana, J.-F. Europe. In *Climate Change 2014: Impacts, Adaptation, and Vulnerability. Part B: Regional Aspects. Contribution of Working Group II to the Fifth Assessment Report of the Intergovernmental Panel on Climate Change*; Barros, V.R., Field, C.B., Dokken, D.J., Mastrandrea, M.D., Mach, K.J., Bilir, T.E., Chatterjee, M., Ebi, K.L., Estrada, Y.O., Genova, R.C., et al., Eds.; Cambridge University Press: Cambridge, UK; New York, NY, USA, 2014; pp. 1267–1326.
- Fischer, E.M.; Schar, C.R. Consistent geographical patterns of changes in high-impact European heatwaves. *Nat. Geosci.* **2010**, *3*, 398–403. [[CrossRef](#)]
- Jacob, D.; Kotova, L.; Teichmann, C.; Sobolowski, S.P.; Vautard, R.; Donnelly, C.; Koutroulis, A.G.; Grillakis, M.G.; Tsanis, I.K.; Damm, A.; et al. Climate impacts in Europe Under +1.5 °C global warming. *Earths Future* **2018**, *6*, 264–285. [[CrossRef](#)]
- Hoegh-Guldberg, O.; Jacob, D.; Taylor, M.; Bindi, M.; Brown, S.; Camilloni, I.; Diedhiou, A.; Djalante, R.; Ebi, K.L.; Engelbrecht, F.; et al. Impacts of 1.5 °C Global Warming on Natural and Human Systems. In *Global Warming of 1.5 °C, An IPCC Special Report on the Impacts of Global Warming of 1.5 °C above Pre-Industrial Levels and Related Global Greenhouse Gas Emission Pathways, in the Context of Strengthening the Global Response to the Threat of Climate Change, Sustainable Development, and Efforts to Eradicate Poverty*; Masson-Delmotte, V., Zhai, P., Pörtner, H.-O., Roberts, D., Skea, J., Shukla, P.R., Pirani, A., Moufouma-Okia, W., Péan, C., Pidcock, R., et al., Eds.; IPCC: Geneva, Switzerland, 2018.
- Geletič, J.; Lehnert, M.; Savić, S.; Milošević, D. Modelled spatiotemporal variability of outdoor thermal comfort in local climate zones of the city of Brno, Czech Republic. *Sci. Total Environ.* **2018**, *624*, 385–395. [[CrossRef](#)] [[PubMed](#)]
- Gál, T.; Mahó, S.I.; Skarbit, N.; Unger, J. Numerical modelling for analysis of the effect of different urban green spaces on urban heat load patterns in the present and in the future. *Comput. Environ. Urban Syst.* **2021**, *87*, 101600. [[CrossRef](#)]
- Voogt, J.; Oke, T. Thermal remote sensing of urban climates. *Remote Sens. Environ.* **2003**, *86*, 370–384. [[CrossRef](#)]
- WMO. *2019 Concludes a Decade of Exceptional Global Heat and High-Impact Weather*; WMO: Geneva, Switzerland, 2019; Available online: <https://public.wmo.int/en/media/press-release/2019-concludes-decade-of-exceptional-global-heat-and-high-impact-weather> (accessed on 10 October 2020).
- Eckstein, D.; Künzel, V.; Schäfer, L.; Wings, M. *Global Climate Risk Index 2020: Who Suffers Most from Extreme Weather Events? Weather-Related Loss Events in 2018 and 1999 to 2018*; Germanwatch e.V.: Bonn, Germany, 2019; p. 44. Available online: <https://www.germanwatch.org/en/cri> (accessed on 11 October 2020).
- UN. *World Urbanization Prospects—The 2014 Revision*; UN Department of Economic and Social Affairs: New York, NY, USA, 2014.
- Seto, K.C.; Güneralp, B.; Hutya, L.R. Global forecasts of urban expansion to 2030 and direct impacts on biodiversity and carbon pools. *Proc. Natl. Acad. Sci. USA* **2012**, *109*, 16083–16088. [[CrossRef](#)]
- Muller, C.L.; Chapman, L.; Grimmond, C.S.B.; Young, D.T.; Cai, X. Sensors and the city: A review of urban meteorological networks. *Int. J. Clim.* **2013**, *33*, 1585–1600. [[CrossRef](#)]
- Baccini, M.; Biggeri, A.; Accetta, G.; Kosatsky, T.; Katsouyanni, K.; Analitis, A.; Anderson, H.R.; Bisanti, L.D.; Ippoliti, D.; Danova, J.; et al. Heat effects on mortality in 15 European Cities. *Epidemiology* **2008**, *19*, 711–719. [[CrossRef](#)]
- Wilhelmi, O.V.; Hayden, M.H. Connecting people and place: A new framework for reducing urban vulnerability to extreme heat. *Environ. Res. Lett.* **2010**, *5*, 014021. [[CrossRef](#)]
- Gasparrini, A.; Guo, Y.; Hashizume, M.; Lavigne, E.; Zanobetti, A.; Schwartz, J.; Tobias, A.; Tong, S.; Rocklöv, J.; Forsberg, B.; et al. Mortality risk attributable to high and low ambient temperature: A multicountry observational study. *Lancet* **2015**, *386*, 369–375. [[CrossRef](#)]
- Gehrels, H.; van der Meulen, S.; Schasfoort, F.; Bosch, P.; Broolsma, R.; van Dinther, D.; Geerling, G.; Goossen, M.; Jacobs, C.; de Jong, M.; et al. *Designing Green and Blue Infrastructure to Support Healthy Urban Living*; TO2 Federatie: Utrecht, The Netherlands, 2016; p. 109.
- Arsenović, D.; Savić, S.; Lužanin, Z.; Radić, I.; Milošević, D.; Arsić, M. Heat-related mortality as an indicator of population vulnerability in a mid-sized Central European city (Novi Sad, Serbia, summer 2015). *Geogr. Pannonica* **2019**, *23*, 204–215. [[CrossRef](#)]
- Wouters, H.; De Ridder, K.; Poelmans, L.; Willems, P.; Brouwers, J.; Hosseinzadehtalaei, P.; Tabari, H.; Broucke, S.V.; Van Lipzig, N.P.M.; Demuzere, M. Heat stress increase under climate change twice as large in cities as in rural areas: A study for a densely populated midlatitude maritime region. *Geophys. Res. Lett.* **2017**, *44*, 8997–9007. [[CrossRef](#)]
- EU. *Human Health Impacts of Climate Change in Europe—JRC Technical Reports*; European Commission, Joint Research Centre, Institute for Prospective Technological Studies: Seville, Spain, 2014; p. 32.
- Kamal-Chaoui, L.; Robert, A. Competitive Cities and climate change. *OECD Reg. Dev. Work. Pap.* **2009**. [[CrossRef](#)]
- Oke, T.; Mills, G.; Christen, A.; Voogt, J. *Urban Climates*; Cambridge University Press: Cambridge, UK, 2017.
- Oke, T.R. The energetic basis of the urban heat island. *Q. J. R. Meteorol. Soc.* **1982**, *108*, 1–24. [[CrossRef](#)]
- Unger, J. Heat island intensity with different meteorological conditions in a medium-sized town: Szeged, Hungary. *Theor. Appl. Clim.* **1996**, *54*, 147–151. [[CrossRef](#)]
- Peng, S.; Piao, S.; Ciais, P.; Friedlingstein, P.; Otle, C.; Bréon, F.-M.; Nan, H.; Zhou, L.; Myneni, R.B. Surface urban heat island across 419 global big cities. *Environ. Sci. Technol.* **2011**, *46*, 696–703. [[CrossRef](#)] [[PubMed](#)]
- Lehnert, M.; Geletič, J.; Husák, J.; Vysoudil, M. Urban field classification by “local climate zones” in a medium-sized Central European city: The case of Olomouc (Czech Republic). *Theor. Appl. Clim.* **2015**, *122*, 531–541. [[CrossRef](#)]

26. Lelovics, E.; Unger, J.; Savić, S.; Gál, T.; Milošević, D.; Gulyás, Á.; Marković, V.; Arsenović, D.; Gál, C.V. Intra-urban temperature observations in two Central European cities: A summer study. *Időjárás* **2016**, *120*, 283–300.
27. Zhou, B.; Rybski, D.; Kropp, J.P. The role of city size and urban form in the surface urban heat island. *Sci. Rep.* **2017**, *7*, 4791. [[CrossRef](#)]
28. Hutcheon, R.J.; Johnson, R.H.; Lowry, W.P.; Black, C.H.; Hadley, D. Observations of the urban heat island in a small city. *Bull. Am. Meteorol. Soc.* **1967**, *48*, 7–9. [[CrossRef](#)]
29. Kopec, R.J. Further observations of the urban heat island in a small city. *Bull. Am. Meteorol. Soc.* **1970**, *51*, 602–606. [[CrossRef](#)]
30. Blazejczyk, K.; Bakowska, M.; Wieclaw, M. Urban heat island in large and small cities. In Proceedings of the 6th International Conference on Urban Climate, Göteborg, Sweden, 12–16 June 2006; pp. 794–797.
31. Ellena, M.; Breil, M.; Soriani, S. The heat-health nexus in the urban context: A systematic literature review exploring the socio-economic vulnerabilities and built environment characteristics. *Urban Clim.* **2020**, *34*, 100676. [[CrossRef](#)]
32. Bokwa, A.; Hajto, M.J.; Walawender, J.P.; Szymanowski, M. Influence of diversified relief on the urban heat island in the city of Kraków, Poland. *Theor. Appl. Clim.* **2015**, *122*, 365–382. [[CrossRef](#)]
33. Stewart, I.D.; Oke, T.R. Local climate zones for urban temperature studies. *Bull. Am. Meteorol. Soc.* **2012**, *93*, 1879–1900. [[CrossRef](#)]
34. Ellefsen, R. Mapping and measuring buildings in the canopy boundary layer in ten U.S. cities. *Energy Build.* **1991**, *16*, 1025–1049. [[CrossRef](#)]
35. Oke, T.R. *Initial Guidance to Obtain Representative Meteorological Observations at Urban Sites*; IOM Rep. WMO/TD-No. 1250; WMO: Geneva, Switzerland, 2004; p. 47. Available online: www.wmo.int/pages/prog/www/IMOP/publications/IOM-81/IOM-81-UrbanMetObs.pdf (accessed on 12 October 2020).
36. Oke, T.R. *Urban Observations. Guide to Meteorological Instruments and Methods of Observation, Part II of Observing Systems*, 7th ed.; II-11-1–II-11-25; WMO: Geneva, Switzerland, 2008.
37. Oke, T.R. *Guide to Instruments and Methods of Observation*; WMO: Geneva, Switzerland, 2018; Volume III—Observing Systems, p. 426.
38. Anderson, J.R.; Hardy, E.E.; Roach, J.T.; Witmer, R.E. A land use and land cover classification system for use with remote sensor data. *Prof. Pap.* **1976**, *964*, 28. [[CrossRef](#)]
39. Auer, A.H. Correlation of land use and cover with meteorological anomalies. *J. Appl. Meteor.* **1978**, *17*, 636–643. [[CrossRef](#)]
40. Häubi, F.; Roth, U. Wechselwirkung zwischen der Siedlungsstruktur und Wärmeversorgungssystemen [Interaction between settlement structure and heating supply systems]. *Forschungsprojekt* **1980**, 270. [[CrossRef](#)]
41. Brunn, S.D.; Williams, J.F. *Cities of the World: World Regional Urban Development*; Harper and Row: New York, NY, USA, 1983; p. 506.
42. Hoyle, B.S.; O'Connor, A. The African city. *Geogr. J.* **1984**, *150*, 253. [[CrossRef](#)]
43. Vance, J.E., Jr. *The Continuous City: Urban Morphology in Western Civilization*; John Hopkins University Press: Baltimore, MD, USA, 1990; p. 552.
44. Kostof, S. *The City Shaped: Urban Patterns and Meanings through History*; Thames and Hudson: London, UK, 1991; p. 352.
45. Wieringa, J. Representative roughness parameters for homogeneous terrain. *Bound. Layer Meteorol.* **1993**, *63*, 323–363. [[CrossRef](#)]
46. Potter, R.B.; Lloyd-Evans, S. *The City in the Developing World*; Longman: London, UK, 1998; p. 244.
47. Grimmond, C.S.B.; Oke, T.R. Aerodynamic properties of urban areas derived from analysis of surface form. *J. Appl. Meteorol.* **1999**, *38*, 1262–1292. [[CrossRef](#)]
48. Theurer, W. Typical building arrangements for urban air pollution modelling. *Atmos. Environ.* **1999**, *33*, 4057–4066. [[CrossRef](#)]
49. Emmanuel, R.; Loconsole, A. Green infrastructure as an adaptation approach to tackling urban overheating in the Glasgow Clyde Valley Region, UK. *Landsc. Urban Plan.* **2015**, *138*, 71–86. [[CrossRef](#)]
50. Stewart, I.D.; Oke, T.R.; Krayenhoff, E.S. Evaluation of the 'local climate zone' scheme using temperature observations and model simulations. *Int. J. Clim.* **2014**, *34*, 1062–1080. [[CrossRef](#)]
51. Lelovics, E.; Unger, J.; Gál, T.; Gál, C. Design of an urban monitoring network based on Local Climate Zone mapping and temperature pattern modelling. *Clim. Res.* **2014**, *60*, 51–62. [[CrossRef](#)]
52. Bechtel, B.; Alexander, P.J.; Beck, C.; Böhner, J.; Brousse, O.; Ching, J.; Demuzere, M.; Fonte, C.; Gál, T.; Hidalgo, J.; et al. Generating WUDAPT Level 0 data—Current status of production and evaluation. *Urban Clim.* **2019**, *27*, 24–45. [[CrossRef](#)]
53. Feranec, J.; Kopecká, M.; Szatmári, D.; Holec, J.; Šťastný, P.; Pazúr, R.; Bobáľová, H. A review of studies involving the effect of land cover and land use on the urban heat island phenomenon, assessed by means of the MUKLIMO model. *Geografie* **2019**, *124*, 83–101. [[CrossRef](#)]
54. Grant, M.J.; Booth, A. A typology of reviews: An analysis of 14 review types and associated methodologies. *Health Inf. Libr. J.* **2009**, *26*, 91–108. [[CrossRef](#)] [[PubMed](#)]
55. Pullin, A.S.; Stewart, G.B. Guidelines for systematic review in conservation and environmental management. *Conserv. Biol.* **2006**, *20*, 1647–1656. [[CrossRef](#)]
56. Moher, D.; Liberati, A.; Tetzlaff, J.; Altman, D.G.; The PRISMA Group. Preferred reporting items for systematic reviews and meta-analyses: The PRISMA statement. *PLoS Med.* **2009**, *6*, e1000097. [[CrossRef](#)]
57. Guo, Y.-M.; Huang, Z.-L.; Guo, J.; Li, H.; Guo, X.-R.; Nkeli, M.J. Bibliometric analysis on smart cities research. *Sustainability* **2019**, *11*, 3606. [[CrossRef](#)]

58. Du, H.; Liu, D.; Lu, Z.; Crittenden, J.; Mao, G.; Wang, S.; Zou, H. Research Development on Sustainable Urban Infrastructure From 1991 to 2017: A Bibliometric Analysis to Inform Future Innovations. *Earths Future* **2019**, *7*, 718–733. [[CrossRef](#)]
59. Yu, D.; Xu, Z.; Wang, X. Bibliometric analysis of support vector machines research trend: A case study in China. *Int. J. Mach. Learn. Cybern.* **2020**, *11*, 715–728. [[CrossRef](#)]
60. Tornay, N.; Schoetter, R.; Bonhomme, M.; Faraut, S.; Masson, V. GENIUS: A methodology to define a detailed description of buildings for urban climate and building energy consumption simulations. *Urban Clim.* **2017**, *20*, 75–93. [[CrossRef](#)]
61. Bocher, E.; Petit, G.; Bernard, J.; Palominos, S. A geoprocessing framework to compute urban indicators: The MApUCE tools chain. *Urban Clim.* **2018**, *24*, 153–174. [[CrossRef](#)]
62. Gardes, T.; Schoetter, R.; Hidalgo, J.; Long, N.; Marquès, E.; Masson, V. Statistical prediction of the nocturnal urban heat island intensity based on urban morphology and geographical factors—An investigation based on numerical model results for a large ensemble of French cities. *Sci. Total Environ.* **2020**, *737*, 139253. [[CrossRef](#)] [[PubMed](#)]
63. Nedkov, S.; Zhiyanski, M.; Dimitrov, S.; Borisova, B.; Popov, A.; Ihtimanski, I.; Yaneva, R.; Nikolov, P.; Bratanova-Doncheva, S. Mapping and assessment of urban ecosystem condition and services using integrated index of spatial structure. *One Ecosyst.* **2017**, *2*, e14499. [[CrossRef](#)]
64. Hu, J.; Ghamisi, P.; Zhu, X.X. Feature extraction and selection of Sentinel-1 dual-pol data for global-scale local climate zone classification. *ISPRS Int. J. Geo-Inf.* **2018**, *7*, 379. [[CrossRef](#)]
65. Bechtel, B.; Demuzere, M.; Mills, G.; Zhan, W.; Sismanidis, P.; Small, C.; Voogt, J. SUHI analysis using local climate zones—A comparison of 50 cities. *Urban Clim.* **2019**, *28*, 100451. [[CrossRef](#)]
66. Demuzere, M.; Bechtel, B.; Middel, A.; Mills, G. Mapping Europe into local climate zones. *PLoS ONE* **2019**, *14*, e0214474. [[CrossRef](#)] [[PubMed](#)]
67. Unger, J.; Savic, S.; Gál, T. Modelling of the annual mean urban heat island pattern for planning of representative urban climate station network. *Adv. Meteorol.* **2011**, *2011*, 398613. [[CrossRef](#)]
68. Bechtel, B.; Daneke, C. Classification of local climate zones based on multiple earth observation data. *IEEE J. Sel. Top. Appl. Earth Obs. Remote Sens.* **2012**, *5*, 1191–1202. [[CrossRef](#)]
69. Stewart, I.D.; Oke, T.R. Newly developed “thermal climate zones” for defining and measuring urban heat island magnitude in the canopy layer. In Proceedings of the 8th Symposium on the Urban Environment, Phoenix, AZ, USA, 11–15 January 2009.
70. Stewart, I.D.; Oke, T.R. Thermal differentiation of local climate zones using temperature observations from urban and rural field sites. In Proceedings of the 9th Symposium on the Urban Environment, Keystone, CO, USA, 2–6 August 2010.
71. Davenport, A.G.; Grimmond, S.B.; Oke, T.R.; Wieringa, J. Estimating the roughness of cities and sheltered country. In Proceedings of the 12th Conference on Applied Climatology, Asheville, NC, USA, 8 May 2000; Volume 96, p. 99.
72. Savić, S.; Milošević, D.; Lazić, L.; Marković, V.; Arsenović, D.; Pavić, D. Classifying urban meteorological stations sites by ‘local climate zones’: Preliminary results for the city of Novi Sad (Serbia). *Geogr. Pannonica* **2013**, *17*, 60–68. [[CrossRef](#)]
73. Wiesner, S.; Eschenbach, A.; Ament, F. Urban air temperature anomalies and their relation to soil moisture observed in the city of Hamburg. *Meteorol. Z.* **2014**, *23*, 143–157. [[CrossRef](#)]
74. Müller, N.; Kuttler, W.; Barlag, A.-B. Counteracting urban climate change: Adaptation measures and their effect on thermal comfort. *Theor. Appl. Climatol.* **2013**, *115*, 243–257. [[CrossRef](#)]
75. Herbel, I.; Croitoru, A.-E.; Rus, I.; Harpa, G.V.; Ciupertea, A.-F. Detection of atmospheric urban heat island through direct measurements in Cluj-Napoca city, Romania. *Hung. Geogr. Bull.* **2016**, *65*, 117–128. [[CrossRef](#)]
76. Pour, T.; Miřijovský, J.; Purket, T. Airborne thermal remote sensing: The case of the city of Olomouc, Czech Republic. *Eur. J. Remote Sens.* **2019**, *52*, 209–218. [[CrossRef](#)]
77. Pour, T.; Voženilek, V. Thermal data analysis for urban climate research: A case study of Olomouc, Czechia. *Geogr. Cassoviensis* **2020**, *14*, 77–91. [[CrossRef](#)]
78. Theeuwes, N.E.; Steeneveld, G.-J.; Ronda, R.J.; Rotach, M.W.; Holtslag, A.A.M. Cool city mornings by urban heat. *Environ. Res. Lett.* **2015**, *10*, 114022. [[CrossRef](#)]
79. Droste, A.M.; Steeneveld, G.J.; Holtslag, A.A.M. Introducing the urban wind island effect. *Environ. Res. Lett.* **2018**, *13*, 094007. [[CrossRef](#)]
80. Geletič, J.; Lehnert, M. GIS-based delineation of local climate zones: The case of medium-sized Central European cities. *Morav. Geogr. Rep.* **2016**, *24*, 2–12. [[CrossRef](#)]
81. Unger, J.; Lelovics, E.; Gál, T. Local Climate Zone mapping using GIS methods in Szeged. *Hung. Geogr. Bull.* **2014**, *63*, 29–41. [[CrossRef](#)]
82. Šećerov, I.; Savić, S.; Milošević, D.; Marković, V.; Bajšanski, I. Development of an automated urban climate monitoring system in Novi Sad (Serbia). *Geogr. Pannonica* **2015**, *19*, 174–183. [[CrossRef](#)]
83. Šećerov, I.B.; Savić, S.M.; Milošević, D.D.; Arsenović, D.M.; Dolinaj, D.M.; Popov, S.B. Progressing urban climate research using a high-density monitoring network system. *Environ. Monit. Assess.* **2019**, *191*, 89. [[CrossRef](#)] [[PubMed](#)]
84. Skarbit, N.; Gal, T.; Unger, J. Airborne surface temperature differences of the different Local Climate Zones in the urban area of a medium sized city. In Proceedings of the 2015 Joint Urban Remote Sensing Event (JURSE), Lausanne, Switzerland, 30 March–1 April 2015; pp. 1–4. [[CrossRef](#)]
85. Unger, J.; Gál, T.M.; Csépe, Z.; Lelovics, E.; Gulyás, Á. Development, data processing and preliminary results of an urban human comfort monitoring and information system. *Iđójárás* **2015**, *119*, 337–354.

86. Gál, T.; Skarbit, N.; Unger, J. Urban heat island patterns and their dynamics based on an urban climate measurement network. *Hung. Geogr. Bull.* **2016**, *65*, 105–116. [CrossRef]
87. Milošević, D.D.; Savić, S.M.; Marković, V.; Arsenović, D.; Šećerov, I. Outdoor human thermal comfort in local climate zones of Novi Sad (Serbia) during heat wave period. *Hung. Geogr. Bull.* **2016**, *65*, 129–137. [CrossRef]
88. Gémes, O.; Tobak, Z.; Van Leeuwen, B. Satellite based analysis of surface urban heat island intensity. *J. Environ. Geogr.* **2016**, *9*, 23–30. [CrossRef]
89. Skarbit, N.; Stewart, I.D.; Unger, J.; Gál, T. Employing an urban meteorological network to monitor air temperature conditions in the 'local climate zones' of Szeged, Hungary. *Int. J. Clim.* **2017**, *37*, 582–596. [CrossRef]
90. Unger, J.; Skarbit, N.; Gál, T. Evaluation of outdoor human thermal sensation of local climate zones based on long-term database. *Int. J. Biometeorol.* **2017**, *62*, 183–193. [CrossRef]
91. Unger, J.; Skarbit, N.; Kovács, A.; Gál, T. Comparison of regional and urban outdoor thermal stress conditions in heatwave and normal summer periods: A case study. *Urban Clim.* **2020**, *32*, 100619. [CrossRef]
92. Savić, S.; Marković, V.; Šećerov, I.; Pavić, D.; Arsenović, D.; Milosevic, D.; Dolinaj, D.; Nagy, I.; Pantelić, M. Heat wave risk assessment and mapping in urban areas: Case study for a midsized Central European city, Novi Sad (Serbia). *Nat. Hazards* **2018**, *91*, 891–911. [CrossRef]
93. Geletič, J.; Lehnert, M.; Savić, S.; Milošević, D. Inter-/intra-zonal seasonal variability of the surface urban heat island based on local climate zones in three central European cities. *Build. Environ.* **2019**, *156*, 21–32. [CrossRef]
94. Geletič, J.; Lehnert, M.; Dobrovolný, P. Modelled spatio-temporal variability of air temperature in an urban climate and its validation: A case study of Brno, Czech Republic. *Hung. Geogr. Bull.* **2016**, *65*, 169–180. [CrossRef]
95. Geletič, J.; Lehnert, M.; Dobrovolný, P. Land surface temperature differences within local climate zones, based on two central European cities. *Remote Sens.* **2016**, *8*, 788. [CrossRef]
96. Lehnert, M.; Geletič, J.; Dobrovolný, P.; Jurek, M. Temperature differences among local climate zones established by mobile measurements in two central European cities. *Clim. Res.* **2018**, *75*, 53–64. [CrossRef]
97. Lehnert, M.; Kubeček, J.; Geletič, J.; Jurek, M.; Frajer, J. Identifying hot and cool spots in the city centre based on bicycle measurements: The case of Olomouc, Czech Republic. *Geogr. Pannonica* **2018**, *22*, 230–240. [CrossRef]
98. Geletič, J.; Lehnert, M.; Dobrovolný, P.; Žuvela-Aloise, M. Spatial modelling of summer climate indices based on local climate zones: Expected changes in the future climate of Brno, Czech Republic. *Clim. Chang.* **2019**, *152*, 487–502. [CrossRef]
99. Rodler, A.; Leduc, T. Local climate zone approach on local and micro scales: Dividing the urban open space. *Urban Clim.* **2019**, *28*, 100457. [CrossRef]
100. Oliveira, A.; Lopes, A.; Niza, S. Local climate zones in five southern European cities: An improved GIS-based classification method based on Copernicus data. *Urban Clim.* **2020**, *33*, 100631. [CrossRef]
101. WUDAPT. World Urban Database and Access Portal Tools. Available online: <http://www.wudapt.org/> (accessed on 15 December 2020).
102. Bechtel, B.; Alexander, P.J.; Böhner, J.; Ching, J.; Conrad, O.; Feddema, J.; Mills, G.; See, L.; Stewart, I. Mapping local climate zones for a worldwide database of the form and function of cities. *ISPRS Int. J. Geo-Inf.* **2015**, *4*, 199–219. [CrossRef]
103. Ching, J.; Mills, G.; Bechtel, B.; See, L.; Feddema, J.; Wang, X.; Ren, C.; Brousse, O.; Martilli, A.; Neophytou, M.; et al. WUDAPT: An Urban Weather, Climate, and Environmental Modeling Infrastructure for the Anthropocene. *Bull. Am. Meteorol. Soc.* **2018**, *99*, 1907–1924. [CrossRef]
104. Conrad, O.; Bechtel, B.; Bock, M.; Dietrich, H.; Fischer, E.; Gerlitz, L.; Wehberg, J.; Wichmann, V.; Böhner, J. System for Automated Geoscientific Analyses (SAGA) v. 2.1. *Geosci. Model Dev.* **2015**, *8*, 1991–2007. [CrossRef]
105. Verdonck, M.-L.; Okujeni, A.; van der Linden, S.; Demuzere, M.; De Wulf, R.; Van Coillie, F. Influence of neighbourhood information on 'Local Climate Zone' mapping in heterogeneous cities. *Int. J. Appl. Earth Obs. Geo-Inf.* **2017**, *62*, 102–113. [CrossRef]
106. Verdonck, M.-L.; Demuzere, M.; Hooyberghs, H.; Beck, C.; Cyrus, J.; Schneider, A.; Dewulf, R.; Van Coillie, F. The potential of local climate zones maps as a heat stress assessment tool, supported by simulated air temperature data. *Landsc. Urban Plan.* **2018**, *178*, 183–197. [CrossRef]
107. Verdonck, M.-L.; Demuzere, M.; Hooyberghs, H.; Priem, F.; Van Coillie, F. Heat risk assessment for the Brussels capital region under different urban planning and greenhouse gas emission scenarios. *J. Environ. Manag.* **2019**, *249*, 109210. [CrossRef]
108. Richard, Y.; Emery, J.; Dudek, J.; Pergaud, J.; Chateau-Smith, C.; Zito, S.; Rega, M.; Vairet, T.; Castel, T.; Thévenin, T.; et al. How relevant are local climate zones and urban climate zones for urban climate research? Dijon (France) as a case study. *Urban Clim.* **2018**, *26*, 258–274. [CrossRef]
109. Qiu, C.; Schmitt, M.; Mou, L.; Ghamisi, P.; Zhu, X.X. Feature importance analysis for local climate zone classification using a residual convolutional neural network with multi-source datasets. *Remote Sens.* **2018**, *10*, 1572. [CrossRef]
110. Droste, A.M.; Heusinkveld, B.G.; Fenner, D.; Steeneveld, G. Assessing the potential and application of crowdsourced urban wind data. *Q. J. R. Meteorol. Soc.* **2020**, *146*, 2671–2688. [CrossRef]
111. Skarbit, N.; Gál, T. Projection of intra-urban modification of night-time climate indices during the 21st century. *Hung. Geogr. Bull.* **2016**, *65*, 181–193. [CrossRef]
112. Fenner, D.; Meier, F.; Bechtel, B.; Otto, M.; Scherer, D. Intra and inter 'local climate zone' variability of air temperature as observed by crowdsourced citizen weather stations in Berlin, Germany. *Meteorol. Z.* **2017**, *26*, 525–547. [CrossRef]

113. Fenner, D.; Holtmann, A.; Meier, F.; Langer, I.; Scherer, D. Contrasting changes of urban heat island intensity during hot weather episodes. *Environ. Res. Lett.* **2019**, *14*, 124013. [\[CrossRef\]](#)
114. Beck, C.; Straub, A.; Breitner, S.; Cyrus, J.; Philipp, A.; Rathmann, J.; Schneider, A.; Wolf, K.; Jacobeit, J. Air temperature characteristics of local climate zones in the Augsburg urban area (Bavaria, southern Germany) under varying synoptic conditions. *Urban Clim.* **2018**, *25*, 152–166. [\[CrossRef\]](#)
115. Bokwa, A.; Geletič, J.; Lehnert, M.; Žuvela-Aloise, M.; Hollósi, B.; Gál, T.; Skarbit, N.; Dobrovolný, P.; Hajto, M.J.; Kielar, R.; et al. Heat load assessment in Central European cities using an urban climate model and observational monitoring data. *Energy Build.* **2019**, *201*, 53–69. [\[CrossRef\]](#)
116. Dian, C.; Pongrácz, R.; Dezső, Z.; Bartholy, J. Annual and monthly analysis of surface urban heat island intensity with respect to the local climate zones in Budapest. *Urban Clim.* **2020**, *31*, 100573. [\[CrossRef\]](#)
117. Fricke, C.; Pongrácz, R.; Gál, T.; Savić, S.; Unger, J. Using local climate zones to compare remotely sensed surface temperatures in temperate cities and hot desert cities. *Morav. Geogr. Rep.* **2020**, *28*, 48–60. [\[CrossRef\]](#)
118. Rathmann, J.; Beck, C.; Flutura, S.; Seiderer, A.; Aslan, I.; André, E. Towards quantifying forest recreation: Exploring outdoor thermal physiology and human well-being along exemplary pathways in a central European urban forest (Augsburg, SE-Germany). *Urban For. Urban Green.* **2020**, *49*, 126622. [\[CrossRef\]](#)
119. Vuckovic, M.; Hammerberg, K.; Mahdavi, A. Urban weather modeling applications: A Vienna case study. *Build. Simul.* **2019**, *13*, 99–111. [\[CrossRef\]](#)
120. Brousse, O.; Martilli, A.; Foley, M.; Mills, G.; Bechtel, B. WUDAPT, an efficient land use producing data tool for mesoscale models? Integration of urban LCZ in WRF over Madrid. *Urban Clim.* **2016**, *17*, 116–134. [\[CrossRef\]](#)
121. Yoo, C.; Han, D.; Im, J.; Bechtel, B. Comparison between convolutional neural networks and random forest for local climate zone classification in mega urban areas using Landsat images. *ISPRS J. Photogramm.* **2019**, *157*, 155–170. [\[CrossRef\]](#)
122. Zonato, A.; Martilli, A.; Di Sabatino, S.; Zardi, D.; Giovannini, L. Evaluating the performance of a novel WUDAPT averaging technique to define urban morphology with mesoscale models. *Urban Clim.* **2020**, *31*, 100584. [\[CrossRef\]](#)
123. Danylo, O.; See, L.; Bechtel, B.; Schepaschenko, D.; Fritz, S. Contributing to WUDAPT: A local climate zone classification of two cities in Ukraine. *IEEE J. Sel. Top. Appl. Earth Obs. Remote Sens.* **2016**, *9*, 1841–1853. [\[CrossRef\]](#)
124. Gholami, R.M.; Beck, C. Towards the determination of driving factors of varying LST-LCZ relationships: A case study over 25 cities. *Geogr. Pannonica* **2019**, *23*, 289–307. [\[CrossRef\]](#)
125. Demuzere, M.; Bechtel, B.; Mills, G. Global transferability of local climate zone models. *Urban Clim.* **2019**, *27*, 46–63. [\[CrossRef\]](#)
126. Fonte, C.C.; Lopes, P.; See, L.; Bechtel, B. Using OpenStreetMap (OSM) to enhance the classification of local climate zones in the framework of WUDAPT. *Urban Clim.* **2019**, *28*, 100456. [\[CrossRef\]](#)
127. Oxoli, D.; Ronchetti, G.; Minghini, M.; Molinari, M.E.; Lotfian, M.; Sona, G.; Brovelli, M.A. Measuring urban land cover influence on air temperature through multiple Geo-Data—The case of Milan, Italy. *ISPRS Int. J. Geo-Inf.* **2018**, *7*, 421. [\[CrossRef\]](#)
128. Geis, C.; Leichtle, T.; Wurm, M.; Pelizari, P.A.; Standfus, I.; Zhu, X.X.; So, E.; Siedentop, S.; Esch, T.; Taubenbock, H. Large-area characterization of urban morphology—Mapping of built-up height and density using TanDEM-X and Sentinel-2 data. *IEEE J. Sel. Top. Appl. Earth Obs. Remote Sens.* **2019**, *12*, 2912–2927. [\[CrossRef\]](#)
129. Qiu, C.; Mou, L.; Schmitt, M.; Zhu, X.X. Local climate zone-based urban land cover classification from multi-seasonal Sentinel-2 images with a recurrent residual network. *ISPRS J. Photogramm. Remote Sens.* **2019**, *154*, 151–162. [\[CrossRef\]](#)
130. Rosentreter, J.; Hagensieker, R.; Waske, B. Towards large-scale mapping of local climate zones using multitemporal Sentinel 2 data and convolutional neural networks. *Remote Sens. Environ.* **2020**, *237*, 111472. [\[CrossRef\]](#)
131. Venter, Z.S.; Brousse, O.; Esau, I.; Meier, F. Hyperlocal mapping of urban air temperature using remote sensing and crowdsourced weather data. *Remote Sens. Environ.* **2020**, *242*, 111791. [\[CrossRef\]](#)
132. Hammerberg, K.; Brousse, O.; Martilli, A.; Mahdavi, A. Implications of employing detailed urban canopy parameters for mesoscale climate modelling: A comparison between WUDAPT and GIS databases over Vienna, Austria. *Int. J. Clim.* **2018**, *38*, e1241–e1257. [\[CrossRef\]](#)
133. Hidalgo, J.; Dumas, G.; Masson, V.; Petit, G.; Bechtel, B.; Bocher, E.; Foley, M.; Schoetter, R.; Mills, G. Comparison between local climate zones maps derived from administrative datasets and satellite observations. *Urban Clim.* **2019**, *27*, 64–89. [\[CrossRef\]](#)
134. Alexander, P.J.; Mills, G. Local climate classification and Dublin’s urban heat Island. *Atmosphere* **2014**, *5*, 755–774. [\[CrossRef\]](#)
135. Alexander, P.J.; Mills, G.; Fealy, R. Using LCZ data to run an urban energy balance model. *Urban Clim.* **2015**, *13*, 14–37. [\[CrossRef\]](#)
136. Alexander, P.; Fealy, R.; Mills, G. Simulating the impact of urban development pathways on the local climate: A scenario-based analysis in the greater Dublin region, Ireland. *Landsc. Urban Plan.* **2016**, *152*, 72–89. [\[CrossRef\]](#)
137. Wicki, A.; Parlow, E. Attribution of local climate zones using a multitemporal land use/land cover classification scheme. *J. Appl. Remote Sens.* **2017**, *11*, 026001. [\[CrossRef\]](#)
138. Wicki, A.; Parlow, E.; Feigenwinter, C. Evaluation and modeling of urban heat island intensity in Basel, Switzerland. *Climate* **2018**, *6*, 55. [\[CrossRef\]](#)
139. Molnár, G.; Gyöngyösi, A.Z.; Gál, T. Integration of an LCZ-based classification into WRF to assess the intra-urban temperature pattern under a heatwave period in Szeged, Hungary. *Theor. Appl. Clim.* **2019**, *138*, 1139–1158. [\[CrossRef\]](#)
140. Straub, A.; Berger, K.; Breitner, S.; Cyrus, J.; Geruschkat, U.; Jacobeit, J.; Kühnbach, B.; Kusch, T.; Philipp, A.; Schneider, A.; et al. Statistical modelling of spatial patterns of the urban heat island intensity in the urban environment of Augsburg, Germany. *Urban Clim.* **2019**, *29*, 100491. [\[CrossRef\]](#)

141. Fenner, D.; Meier, F.; Scherer, D.; Polze, A. Spatial and temporal air temperature variability in Berlin, Germany, during the years 2001–2010. *Urban Clim.* **2014**, *10*, 308–331. [[CrossRef](#)]
142. Maharroof, N.; Emmanuel, R.; Thomson, C. Compatibility of local climate zone parameters for climate sensitive street design: Influence of openness and surface properties on local climate. *Urban Clim.* **2020**, *33*, 100642. [[CrossRef](#)]
143. Quanz, J.A.; Ulrich, S.; Fenner, D.; Holtmann, A.; Eimermacher, J. Micro-scale variability of air temperature within a local climate zone in Berlin, Germany, during summer. *Climate* **2018**, *6*, 5. [[CrossRef](#)]
144. Bassett, R.; Cai, X.; Chapman, L.; Heaviside, C.; Thornes, J.E.; Muller, C.L.; Young, D.T.; Warren, E.L. Observations of urban heat island advection from a high-density monitoring network. *Q. J. R. Meteorol. Soc.* **2016**, *142*, 2434–2441. [[CrossRef](#)]
145. Feng, J.; Cai, X.; Chapman, L. Impact of atmospheric conditions and levels of urbanization on the relationship between nocturnal surface and urban canopy heat islands. *Q. J. R. Meteorol. Soc.* **2019**, *145*, 3284–3299. [[CrossRef](#)]
146. Leconte, F.; Bouyer, J.; Claverie, R.; Pétrissans, M. Using local climate zone scheme for UHI assessment: Evaluation of the method using mobile measurements. *Build. Environ.* **2015**, *83*, 39–49. [[CrossRef](#)]
147. Leconte, F.; Bouyer, J.; Claverie, R.; Pétrissans, M. Analysis of nocturnal air temperature in districts using mobile measurements and a cooling indicator. *Theor. Appl. Clim.* **2016**, *130*, 365–376. [[CrossRef](#)]
148. Leconte, F.; Bouyer, J.; Claverie, R. Nocturnal cooling in Local Climate Zone: Statistical approach using mobile measurements. *Urban Clim.* **2020**, *33*, 100629. [[CrossRef](#)]
149. Wouters, H.; Demuzere, M.; Blahak, U.; Fortuniak, K.; Maiheu, B.; Camps, J.; Tielemans, D.; Van Lipzig, N.P.M. The efficient urban canopy dependency parametrization (SURY) v1.0 for atmospheric modelling: Description and application with the COSMO-CLM model for a Belgian summer. *Geosci. Model Dev.* **2016**, *9*, 3027–3054. [[CrossRef](#)]
150. Arnds, D.; Böhner, J.; Bechtel, B. Spatio-temporal variance and meteorological drivers of the urban heat island in a European city. *Theor. Appl. Clim.* **2017**, *128*, 43–61. [[CrossRef](#)]
151. Gonçalves, A.; Ornellas, G.; Ribeiro, A.C.; Maia, F.; Rocha, A.; Feliciano, M. Urban cold and heat island in the city of Bragança (Portugal). *Climate* **2018**, *6*, 70. [[CrossRef](#)]
152. McRae, I.; Freedman, F.R.; Rivera, A.; Li, X.; Dou, J.; Cruz, I.; Ren, C.; Dronova, I.; Fraker, H.; Bornstein, R. Integration of the WUDAPT, WRF, and ENVI-met models to simulate extreme daytime temperature mitigation strategies in San Jose, California. *Build. Environ.* **2020**, *184*, 107180. [[CrossRef](#)]
153. Vázquez-Jiménez, R.; Romero-Calcerrada, R.; Ramos-Bernal, R.N.; Arrogante-Funes, P.; Novillo, C.J. Topographic correction to landsat imagery through slope classification by applying the SCS + C method in mountainous forest areas. *ISPRS Int. J. Geoinf.* **2017**, *6*, 287. [[CrossRef](#)]
154. Bechtel, B.; Demuzere, M.; Sismanidis, P.; Fenner, D.; Brousse, O.; Beck, C.; Van Coillie, F.; Conrad, O.; Keramitsoglou, I.; Middel, A.; et al. Quality of crowdsourced data on urban morphology—The Human Influence Experiment (HUMINEX). *Urban Sci.* **2017**, *1*, 15. [[CrossRef](#)]
155. Kaloustian, N.; Bechtel, B. Local climatic zoning and urban heat island in Beirut. *Procedia Eng.* **2016**, *169*, 216–223. [[CrossRef](#)]
156. Bechtel, B.; See, L.; Mills, G.; Foley, M. Classification of local climate zones using SAR and multispectral data in an arid environment. *IEEE J. Sel. Top. Appl. Earth Obs. Remote Sens.* **2016**, *9*, 3097–3105. [[CrossRef](#)]
157. Mills, G.; Bechtel, B.; Ching, J.; See, L.; Feddema, J.; Foley, M.; Alexander, P.; O'Connor, M. An Introduction to the WUDAPT Project. In Proceedings of the 9th International Conference on Urban Climate ICUC, Toulouse, France, 20–24 July 2015.
158. Middel, A.; Lukaszczuk, J.; Maciejewski, R.; Demuzere, M.; Roth, M. Sky View Factor footprints for urban climate modeling. *Urban Clim.* **2018**, *25*, 120–134. [[CrossRef](#)]
159. Middel, A.; Lukaszczuk, J.; Zakrzewski, S.; Arnold, M.; Maciejewski, R. Urban form and composition of street canyons: A human-centric big data and deep learning approach. *Landsc. Urban Plan.* **2019**, *183*, 122–132. [[CrossRef](#)]
160. Xu, Y.; Ren, C.; Ma, P.; Ho, J.; Wang, W.; Lau, K.K.-L.; Lin, H.; Ng, E. Urban morphology detection and computation for urban climate research. *Landsc. Urban Plan.* **2017**, *167*, 212–224. [[CrossRef](#)]
161. Kaloustian, N.; Tamminga, M.; Bechtel, B. Local climate zones and annual surface thermal response in a Mediterranean city. In Proceedings of the 2017 Joint Urban Remote Sensing Event (JURSE), Dubai, United Arab Emirates, 6–8 March 2017; pp. 1–4.
162. Tuia, D.; Moser, G.; Le Saux, B.; Bechtel, B.; See, L. 2017 IEEE GRSS data fusion contest: Open data for global multimodal land use classification [technical committees]. *IEEE Geosci. Remote Sens.* **2017**, *5*, 70–73. [[CrossRef](#)]
163. Gorelick, N.; Hancher, M.; Dixon, M.; Ilyushchenko, S.; Thau, D.; Moore, R. Google Earth engine: Planetary-scale geospatial analysis for everyone. *Remote Sens. Environ.* **2017**, *202*, 18–27. [[CrossRef](#)]
164. Wang, D.; Jiang, P.; Wang, G.; Wang, D. Urban extent enhances extreme precipitation over the Pearl River Delta, China. *Atmos. Sci. Lett.* **2015**, *16*, 310–317. [[CrossRef](#)]
165. Burić, D.; Doderović, M. Precipitation, humidity and cloudiness in Podgorica (Montenegro) during the period 1951–2018. *Geogr. Pannonica* **2019**, *23*, 233–244. [[CrossRef](#)]
166. Milošević, D.; Kresoja, M.; Savić, S.; Lužanin, Z. Intra-urban analysis of relative humidity and its cross-correlation with air temperature in Centra-european city. In Proceedings of the 10th International Conference on Urban Climate (ICUC10) with the 14th Symposium on the Urban Environment (SUE), New York, NY, USA, 6–10 August 2018; p. 5.
167. Schnell, I.; Cohen, P.; Mandelmlch, M.; Potchter, O. Portable—trackable methodologies for measuring personal and place exposure to nuisances in urban environments: Towards a people oriented paradigm. *Comput. Environ. Urban Syst.* **2021**, *86*, 101589. [[CrossRef](#)]

-
168. Middel, A.; Krayenhoff, E.S. Micrometeorological determinants of pedestrian thermal exposure during record-breaking heat in Tempe, Arizona: Introducing the MaRTy observational platform. *Sci. Total Environ.* **2019**, *687*, 137–151. [[CrossRef](#)]
 169. Hidalgo, J.; Lemonsu, A.; Masson, V. Between progress and obstacles in urban climate interdisciplinary studies and knowledge transfer to society. *Ann. N. Y. Acad. Sci.* **2019**, *1436*, 5–18. [[CrossRef](#)] [[PubMed](#)]
 170. Baklanov, A.; Grimmond, C.; Carlson, D.; Terblanche, D.; Tang, X.; Bouchet, V.; Lee, B.; Langendijk, G.; Kolli, R.; Hovsepyan, A. From urban meteorology, climate and environment research to integrated city services. *Urban Clim.* **2018**, *23*, 330–341. [[CrossRef](#)]